The Influence of Vertical Wind Shear on Hailstorm Development and Structure

By
Alf Carlton Modahl

Department of Atmospheric Science
Colorado State University
Fort Collins, Colorado

Colorado State University

Department of Atmospheric Science

Paper No. 137

THE INFLUENCE OF VERTICAL
WIND SHEAR ON HAILSTORM DEVELOPMENT
AND STRUCTURE

by

Alf Carlton Modahl

Department of Atmospheric Science
Colorado State University
Fort Collins, Colorado

March 1969

ABSTRACT

The influence of vertical wind shear on the development and structure of hailstorms occuring in Northeastern Colorado was examined in this study. The availability of hailfall reports from the Colorado State University Cooperative Reporting Network made it possible to classify the days of the summers of 1966, 1967, and 1968 with regard to hail intensity. Categories of hail intensity ranging from no hail to heavy hail were established.

In order to portray the nature of wind shear in this region, three-year mean profiles of windspeed and direction versus hail intensity were prepared. In addition, mean wind shear magnitudes for the wind field above and below 500 mb were computed for the summer of 1967.

The results showed the nature of the directional shearing of the lower atmosphere below 600 mb as well as a gradation of increasing windspeeds at all levels with increase of hail intensity. It was also found that upper level mean wind shear was relatively constant for all of the days of the summer of 1967, while mean wind shear magnitudes between the surface and 500 mb showed that an increase in shear was accompanied by an increase in hail production.

Radar echo motions measured during the summer of 1967 also showed an increase in speed with increasing hail intensity.

Mean profiles of cloud vertical velocity for 20 days of the summer of 1967 were derived from environmental wind and temperature soundings coupled with the storm motion. Aspects of Newton's (1959) hypothesized mechanism of the hydrodynamic interaction between the storm and the environmental winds were followed. The profiles showed the comparative magnitude of the thermal and hydrodynamic contributions to cloud vertical velocity as well as a clear gradation of increasing cloud vertical velocity with increase of hail production.

The cloud vertical velocity profiles showed the capability of supporting large hail at a low level in the cloud.

The effect of precipitation particle accumulations on the derived updraft profiles was examined in order to produce agreement with radar observations which implied vertical velocity maxima beneath the suspected locations of hail accumulations. It was shown that the superposition of reasonable concentrations of precipitation particles on the derived updraft indeed produced such profiles.

Alf Carlton Modahl
Atmospheric Science Department
Colorado State University
March, 1969

ACKNOWLEDGEMENTS

TABLE OF CONTENTS

List of Tables

List of Figures

I. INTRODUCTION

Pronounced vertical wind shear, implying high winds aloft, is generally cited as being one of the more important agencies operating to intensify convective storms and lead to the production of widespread, damaging hail. Wind shear, defined by Huschke (1959) as "The local variation of the wind vector, or any of its components in a given direction," is manifested in any vertical plane as either a change in direction of the wind with height, or a change in speed of the wind with height, or both, as is frequently the case in the lower levels. Above 700-600 mb the wind is often nearly constant in direction with height; therefore references to wind shear aloft are generally addressed to the increase of wind speed with height only.

The question of the degree of influence of wind shear on hail production has engendered research interest in many areas of the world affected by hail. Colorado State University, (CSU) located in one of the major hail-prone areas of the world, operates a cooperative hail reporting network which has made it possible to stratify hail events in terms of relative hail intensity.

This capability, combined with the observational data obtained by the CSU hail modification project, has facilitated the present study by making it possible to assess under comparable conditions, certain aspects of the vertical wind shear, the wind field, and the thermal instability.

Recent Research

Studies associating high winds aloft with damaging hail occurrences have been accomplished in France, England, Canada, and the United States. Dessens (1960), in France, concluded from statistical studies of hail events and upper wind reports, that "The presence of a jet stream, or at least a very strong wind at upper levels, is the factor which determines whether or not a thunderstorm situation will transform itself into a heavy destructive hailstorm." In England, Browning and Ludlam (1962), and Ludlum and Macklin (1959) mapped the relationships between regions of vertical wind shear

maxima and specific severe hailstorm occurrences over England and the Continent. These investigators found close correspondence between the positions of the leading portions of the middle-level jet maxima, and the location of the specific storms.

In Canada, Longely and Thompson (1965) studied five years of wind flow and hail occurrence over Alberta. The two authors concluded that major hail is associated with higher winds at 500 mb than that present during minor hail situations. On no hail days the upper winds tended to be light, again lending support to Dessen's conclusions. Schleusener (1962), in the United States, studied the relationship between hail and the upper winds over NE Colorado. He found that a 500 mb westerly wind component maxima moved southward along the 110th meridian in conjunction with hail occurrences. Schleusener also found that higher winds aloft were present on severe hail days. (Schleusener, 1963).

Beckwith (1956) in his studies of Denver area hail occurrences, found the upper-level jet stream crossing Colorado on only 10 per cent of the hail days. Later research increased this number to about 15 per cent (Beckwith, 1960).

Ratner (1961) subjected Dessens' theory to a test using U. S. rawinsonde data, and concluded that "neither the speed of the winds aloft nor the wind shear between 500 and 250 mb appeared to be determining factors in occurrences of hail." This conclusion apparently conflicted with the findings of Dessens. Dessens later pointed out that they were not comparing the same type of categories (Dessens, 1961). Dessens stated that he had classified his thunderstorm days as days either having, or not having, widely destructive heavy hailstorms. The latter category included days ranging from no hail to moderate hail. Ratner, however, divided his days into hail days, and no hail days. The difference between the results of the two studies, Dessens suggested, may have arisen from the differing treatment of the moderate hail days.

Das (1962) developed theoretical support for the view that wind shear aloft favors the growth of hail in thunderstorms building under its influence. He examined the physical implications of this view

by performing computations on the growth of hailstones in a model cloud under vertical wind shear, using Beckwith's (1960) mean Denver hail sounding. Das's model utilized shear to horizontally displace hailstone embryos from the genesis updraft. The displaced hailstone embryos would subsequently encounter another building updraft, thereby lengthening the trajectory and the time of hail growth. Wind shear also prevented the hailstone embryos from being lifted into the glaciated portion of the cloud by the genesis updraft. Further growth would be minimal in this region, and the hailstone embryo would most likely be blown downstream in the anvil.

Das concluded that there was a higher probability of hail with shear; however, the maximum hail size would be greater in clouds without shear, all other things being equal. Das credited wind shear with causing a slower rate of growth by taking the embryo into a portion of the cloud where the liquid water content was probably less.

Russian investigators (Sulakvelidze, 1965) stated that hail forms much more rarely in the absence of shear, which is in accordance with the findings of Das. They suggested, however, that the problem required further study.

While the association of marked vertical wind shear and damaging hailstorms is generally accepted, the question of what is the nature of the mechanism through which vertical wind shear may contribute to hail production has not yet been fully settled.

Dessens (1960) suggested a structure for the hailstorm affected by vertical wind shear. He envisioned a mechanism whereby updraft air reaching the top of the "chimney" was entrained into the horizontal environmental flow. High winds aloft would therefore cause the "chimney" to "draw," increasing the vertical velocity of the updraft. Dessens considered the "chimney" to be the linking factor between the kinetic energy of the high winds aloft, and the energy of thermodynamic origin at low levels.

A more quantitative, theoretical examination of the effect of vertical wind shear on cloud growth was made by Newton (1959). He proposed a mechanism based on the assumption that a large cloud mass acts as an obstacle to the environmental flow at all levels, thereby producing a field of hydrodynamic pressures adjacent to the cloud. These pressures induced vertical movement of the deflected air in a manner to be explained in the section on Procedure and Presentation of Results. In this mechanism the vertical transport of momentum by the updraft-downdraft system served to couple the kinetic energy of the winds aloft to the lower regions of the storm mass.

Objectives of the Present Study

It is the purpose of this paper to show, through the quantitative treatment of hailstorm data collected during the summers of 1966, 1967, and 1968 in Northeastern Colorado, the following:

1. the nature of vertical wind shear in Northeastern Colorado and its relation to hail production.

2. the influence of vertical wind shear on hailstorm structure, following certain aspects of Newton's previously mentioned hypothesis concerning hydrodynamic interactions between storm mass and environmental wind flow.

3. the relative importance of Newton's hypothesized mechanism.

Knowledge of the relative importance of Newton's hypothesized mechanism and its evident effect upon storm structure will permit the drawing of some inferences regarding the establishment, location, and nature of precipitation accumulation regions within the storm.

The model thus projected will prove useful in continuing CSU studies directed toward increased understanding of hailstorm dynamics. This will facilitate the design and implementation of improved hailstorm modification techniques, such as the airborne air-to-cloud rocket seeding system described by Sinclair and Marion (1968).

II.   PROCEDURE AND PRESENTATION OF RESULTS

Summary of the Procedure

The following six paragraphs briefly summarize the procedures followed in this study. The procedures are described in detail in the section on Description of the Computational Procedure.

Hailfall data from three summers, 1966, 1967, and 1968 were classified with regard to hailfall intensity. This permitted stratification of the data of this study.

Mean profiles of windspeed and direction were prepared to show the usual nature of summertime vertical wind shear in Northeastern Colorado. Winds from three summers, 1966, 1967, and 1968 were utilized for this short climatology. The winds were stratified with regard to hail intensity before averaging.

Quantitative values of vertical wind shear for two layers, the lower and upper halves of the troposphere, were computed in order to show the magnitude and vertical distribution of the wind shear. Winds from the summer of 1967 were employed for this purpose. The wind shears were stratified with regard to hail intensity, then averaged.

Twenty days from the summer of 1967 were identified as suitable cases for computing the respective contributions of Newton's (1959) hypothesized mechanism, and the thermal instability, to cloud development and structure. The contributions of these two effects were used to derive rainstorm and hailstorm mean vertical velocity profiles for varying hail intensity categories.

The criteria for selection of the 20 days consisted primarily of the concurrent existence of measurements of radar echo motions, temperature soundings taken prior to any major overturning, and the environmental winds.

The effect of imposed precipitation accumulations on the derived updraft strength was examined in an attempt to match the vertical velocity profiles with radar observations of suspected precipitation accumulation heights.

The Data

The following data applying to Northeastern Colorado was utilized in this study.

Hailfall Reports

CSU operates a cooperative hail reporting network in Northeastern Colorado, and adjacent strips of Wyoming and Nebraska. The area covered is shown in Fig. 1. Cooperating farmers and ranchers report the date and time of hailfall, the location, the duration, the maximum hailstone size, the most common hailstone size, the depth of ground coverage, and other pertinent information. This data has been compiled on punch cards for ready access.

Hailfall reports from the summer hail seasons of 1966, 1967, and 1968 were used to classify those days with regard to hail intensity. A summer hail season was defined to be the period from 1 June through 18 August. The classification scheme is presented in detail in the section on Classification of The Hail Season Days.

There are sparsely populated areas within the CSU hail reporting network where an isolated hailstorm could occur unnoticed. Most of the traveling hailstorms, however, will pass over enough of the cooperators to provide significant information. The effect of subjectivity on the part of the cooperators is minimized by a multiplicity of reports. Table 1 shows the size reporting scheme used by the cooperators, who subjectively rated the hail sizes in terms of familiar objects.

TABLE 1.

Hailsize reporting method used by CSU cooperative hail observers.

Code	Size-inches	Familiar Object
1	1/4 or less	shot
2	between 1/4 and 1/2	pea
3	between 1/2 and 3/4	grape
4	between 1 and 1 1/4	walnut
5	between 1 3/4 and 2	golfball
6	larger than 2	larger than golfball
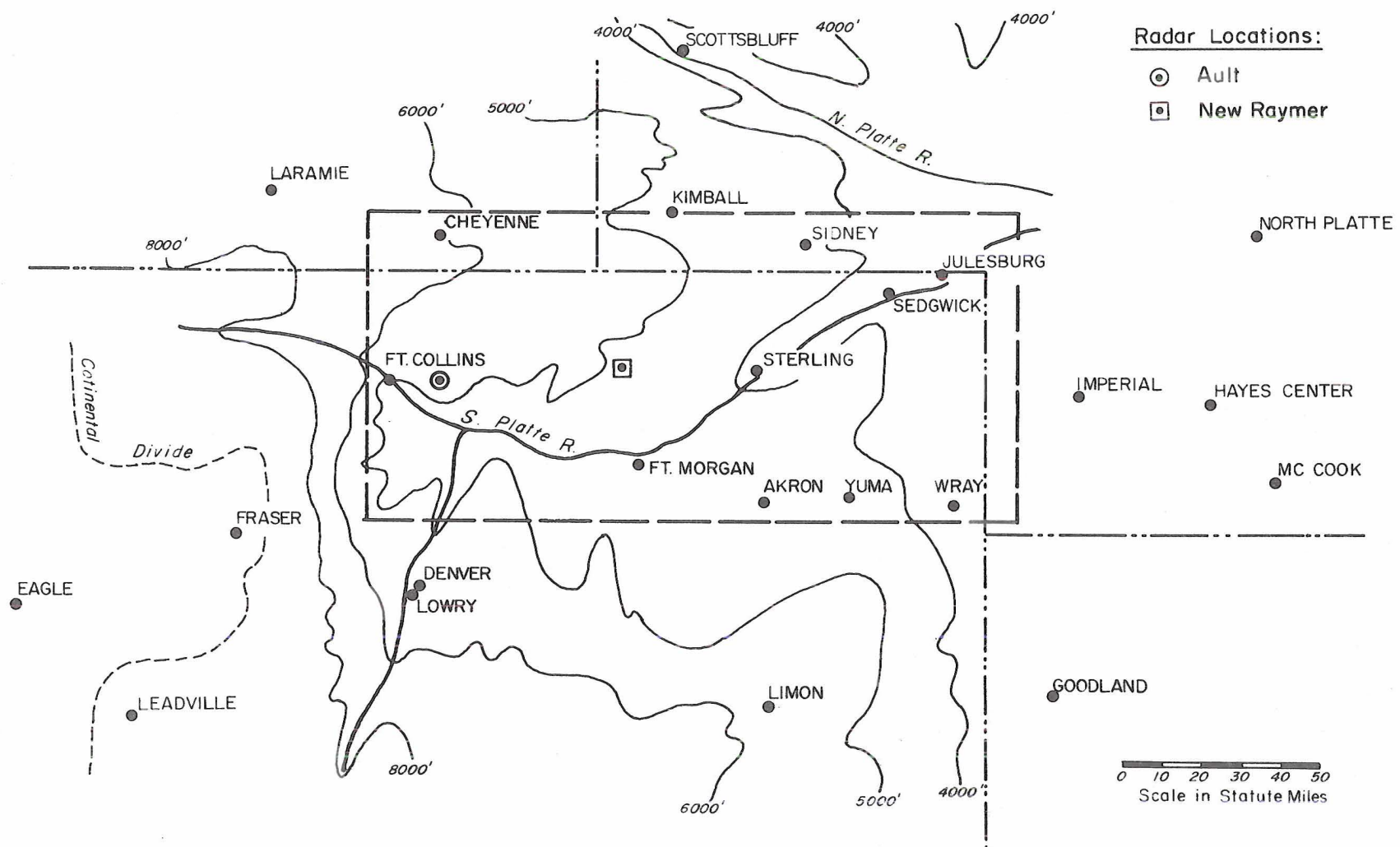
Figure 1. General area of CSU hailstorm studies.

The Environmental Wind Data

Denver 12 MDT rawinsonde winds from the surface to the 100 mb
level for the hail seasons of 1966 and 1967, and rawinsonde winds
taken at Fort Collins in 1968 at 12 MDT were used to produce the
three year mean profiles of windspeed and direction. Denver rawin-
sonde reports at 18 MDT from the summer of 1967 were used in the
determination of the relative winds with respect to the moving cloud
masses. The relative winds were used to compute non-hydrostatic
pressures adjacent to the cloud for 20 days of the 1967 hail season.

The Denver 18 MDT winds for the hail season of 1967 were also
used for the purpose of computing mean vertical wind shears for the
entire hail season.

All of the winds used in this study were measured with radio
theodolite tracking equipment. The accuracy of the rawinsonde winds
used in this study are thought to be better than the accuracy
estimated for pilot balloons by Middleton and Spilhaus (1953).
These authors suggested an error of ± 1 mps in speed, and ± 2 degrees
in direction for measurements near the surface. They estimated that
the error would be doubled at 5 km.

Radar Echo Motions

Radar echo motions were required for the determination of the
relative winds with respect to the moving cloud masses on 20 days
of the hail season of 1967. CSU personnel operate an M-33 radar
site located near Ault, Colorado, and participate in the operation
of another M-33 at New Raymer, Colorado. Figure 1 shows the location
of the radars. The radars were operated six days a week during the
summer of 1967.

Overlays of the PPI scopes of the two radars were made at varying
intervals of 10 to 30 minutes during periods of echo activity. Loca-
tions of the centers of the radar echoes on these overlays were
plotted and the motion measured. The technique employed was similar
to that described in the Thunderstorm Project Report (Byers and
Braham, 1949). The error for this technique is estimated to be ± 10

degrees for the echo heading, and ± 2 mps for echo speed. It was generally not possible to discriminate between translation and propagation of the echoes. This was not considered a liability, as it is the average speed of movement of an echo mass which contributes greatly to the magnitude of the relative wind.

Another technique for obtaining storm motion was developed. In some cases plotting of the largest hail size reports from the hail reporting network showed definite hailswaths. Fig. 2 shows the plot of golfball and larger sized hailfall on 7 June 1967. Smaller hail fell in many areas of the network on that day, but only the embedded, heavy hailfall path showed evidence of the passage of a discrete storm mass. It was possible to measure the rate of progression of hailfall onset, and these velocities showed good agreement with velocities measured from the radar scope overlays. Table 2 shows the agreement among the three independent measurements of storm movement. Close correspondence among the measurements is apparent.

TABLE 2.

Comparison of storm motion as observed by three independent methods; two radar installations and the hail reporting network.

Date	Radar-Ault		Radar-New Raymer		Hailswath-	
	dir deg	speed mps	dir deg	speed mps	dir deg	speed mps
7 June 1967	–	–	285	10.7	300	8.5
13	230	14.7	240	12.3	255	14.2
14	–	–	230	19	245	17
17	275	8.4	280	10.5	–	–
18	–	–	–	–	305	15
20	240	15	260	16.5	–	–
22	–	–	270	14	300	14
26	–	–	280	14.5	–	–
27	290	14.7	–	–	–	–
28	290	15	–	–	–	–
1 July	325	9.2	–	–	340	6.6
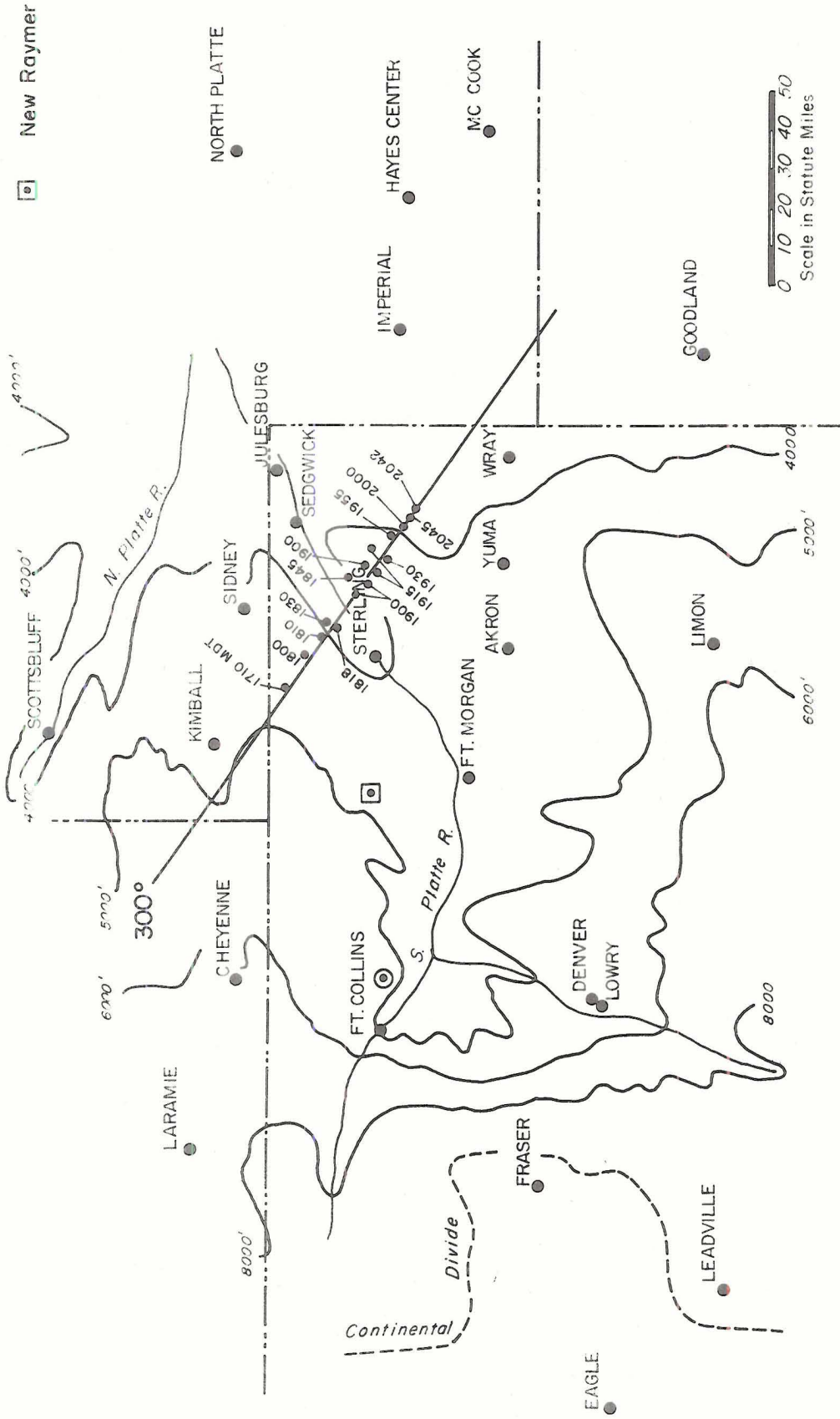
Figure 2. Plot of golfball and larger sized hailfall on 7 June 1967.

Note. This comparison covers only the period of the summer during which significant hailswaths occurred. (Table 2)

Due to inability of the radars to isolate and track embedded hail producing cells within the storm mass on the PPI presentation, it was not possible to correlate surface reports of hail and the motion of particular cells within observed echo masses. In 13 of 15 hailfall cases, however, it was possible to correlate hail reports with the observed echo masses. Detailed hail reports were not available for the two remaining cases.

There was indication of homogeniety of echo speed and direction during a particular day, except in the case of splitting, or converging echoes.

Temperature Soundings

Afternoon soundings taken from the radar site at New Raymer, Colorado, were available for some of the summer days of 1967. Data from the soundings was used to derive the contribution of the thermal instability to cloud development and structure on the 20 case days. Denver 18 MDT rawinsonde data was used whenever New Raymer data was missing. A comparison between corresponding Denver and New Raymer soundings showed generally negligible differences above the cloud base level. The near surface levels usually showed variation. The Denver Soundings utilized, therefore, were adjusted at the surface with the New Raymer afternoon maximum temperatures and the corresponding relative humidities. The Denver upper air station is located approximately 70 statute miles southwest of New Raymer.

The accuracy of rawinsonde temperature measurements has been discussed by Ference (1951). Ference gives the maximum error for temperature measurements in the troposphere as $\pm0.5C$.

Classification of the Hail Season Days

Reports from the CSU cooperative hail reporting network were subjectively analyzed in the following manner. All days on which golfball or larger sized hail fell in the area were considered heavy hail days. Days on which no hail fell were divided into two groups; one, labelled no hail-echoes, consisted of days on which echoes were reported by the radars at Ault and New Raymer, and the

second group consisted of the remaining no hail-no echoes days.
Days on which only scattered reports of the smaller hail sizes
existed were categorized as light hail days. The remaining hail
days were considered to be moderate hail days. The moderate hail
days were characterized by numerous, widespread reports of all
the hail sizes up to, but not including golfball sized hail.

The hail intensity category rating scheme thus attempted to
stratify days primarily by hail size, and secondarily by the
quantity of hail produced. Table 3 presents a summary of the results
of the classification of the hail season days of 1966, 1967, and 1968.
These classifications were used to stratify data for use in all the
comparisons and analyses of this paper.

TABLE 3.

Summary of the results of the classification of the summer
hail season days into five categories of hail intensity.

| Category | Number of Days | | | |
	1966	1967	1968	1966-1968
heavy hail	8	23	5	36
moderate hail	3	10	7	20
light hail	14	14	31	59
no hail-echoes	15	12	16	43
no hail-no echoes	35	20	19	74
total hail days	25	47	43	115
total no hail days	50	32	35	117
total days per season	75	79	78	
three year total days				232

Description of the Computational Procedure

In addition to describing the computational procedure, this sec-
tion of the paper provides a discussion of the governing theoretical
considerations underlying the treatment of data in this study.
Results are presented for reference with the description of each
computational procedure. The results are discussed in detail in
section III.

Preparation of Mean Windspeed Profiles

The winds were considered uni-directional for the purpose of portraying the three year mean windspeed profiles for each hail intensity category. Windspeeds from Denver at 12 MDT, for the hail seasons of 1966 and 1967, and from Fort Collins at 12 MDT, for the 1968 season, were stratified in accordance with the classification scheme summarized in Table 3. Windspeeds at each mandatory pressure level from the surface to 100 mb were averaged arithmetically. Figure 3 shows the resulting profiles.

Preparation of Mean Wind Direction Profiles

In order to portray the usually sheared character of the summer-time wind field in this region, three year mean wind direction profiles for each hail intensity category were prepared. The wind directions at each level were averaged arithmetically. The results are shown in Figure 4. The method employed in producing this characterization of the usually sheared wind field was not sensitive to the possibility of a bi-modal distribution of the upper wind directions. Such information was not required for the purpose of comparing hail intensity categories and portraying the general directional shear of the summertime atmosphere in this region.

Preparation of Mean Vertical Wind Shears

Mean vertical wind shear was computed for the summer of 1967. Denver 18 MDT winds were used in order to include the effect of the higher windspeeds at the surface in the late afternoon. First the shear between the surface and 500 mb was determined. The zonal and meridional component vertical wind shear terms $\frac{\partial u}{\partial p}$ and $\frac{\partial v}{\partial p}$ were evaluated for each day and combined vectorially to yield a shear vector. The magnitudes of the shear vectors for each of the days in a hail intensity category were then averaged without regard for the plane of the shear vector. This produced a mean wind shear magnitude for each hail intensity category.

Mean wind shears were then computed for the upper half of the troposphere using the same technique. The layer 500 to 250 mb was chosen because Ratner (1961) had used this layer in his study of upper level shear magnitudes. Table 4 shows the results.
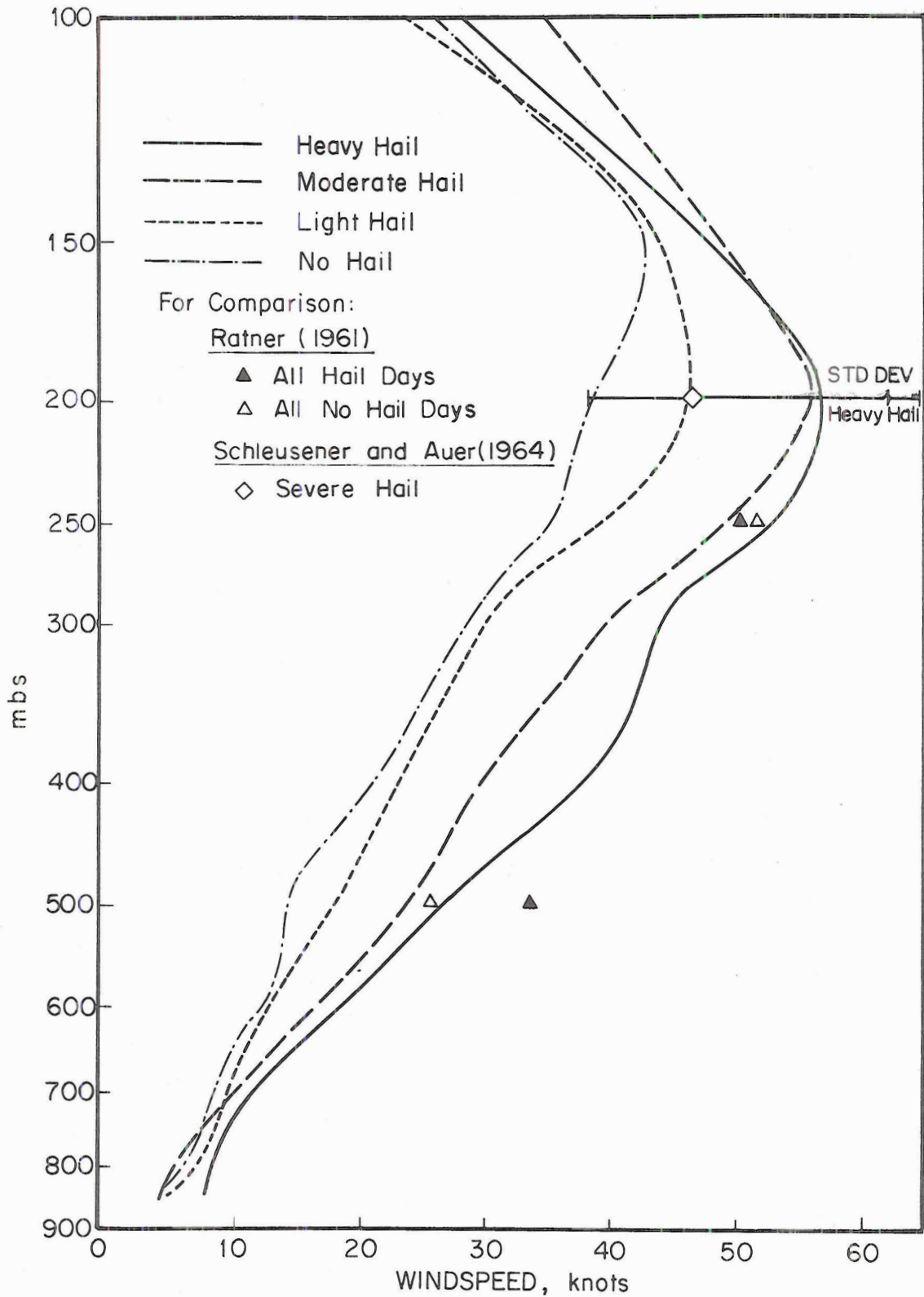
Figure 3. Mean windspeed profiles from the summers of 1966, 1967, and 1968. Denver 12 MDT.
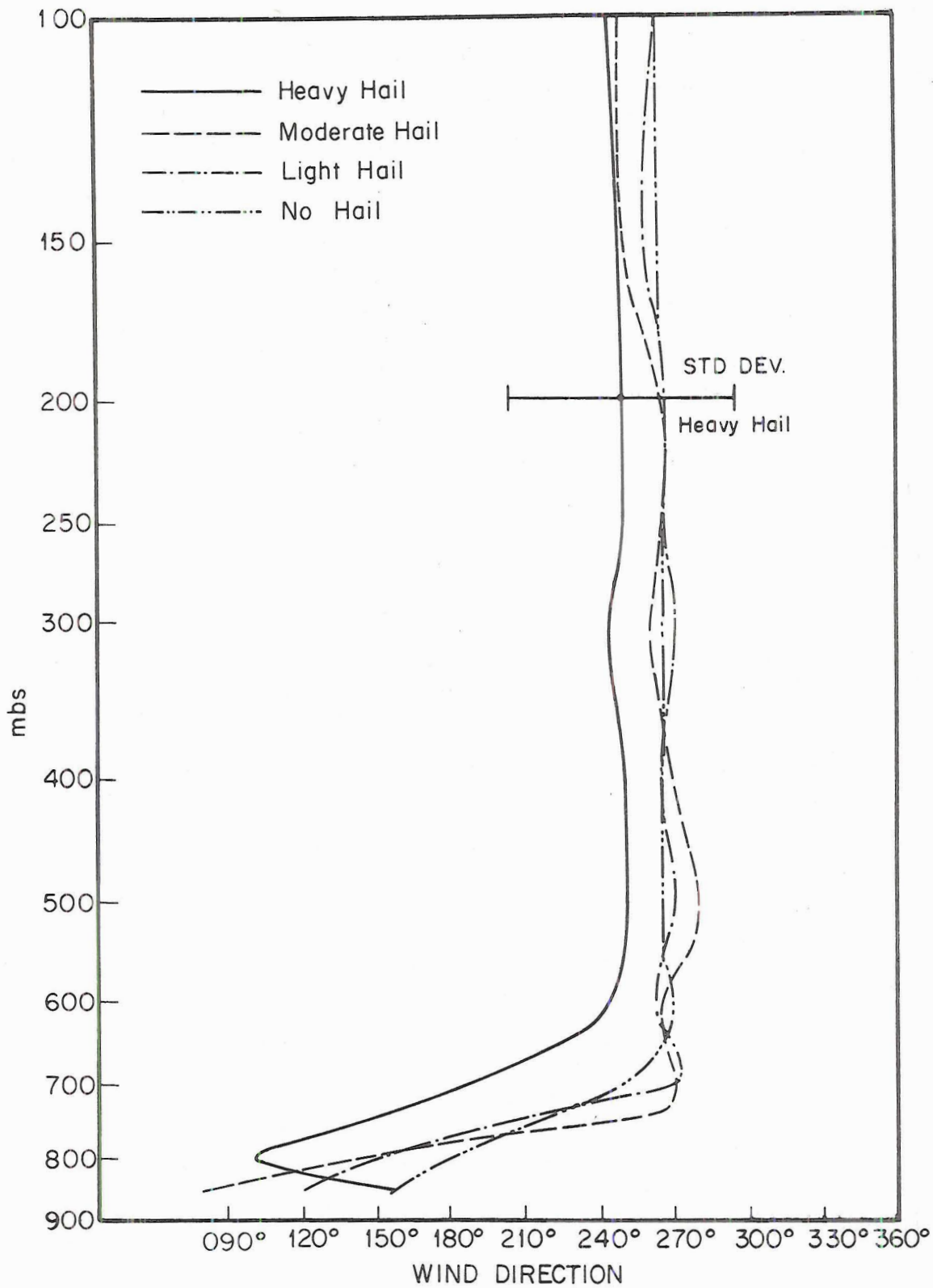
Figure 4. Mean wind direction profiles from the summers of 1966, 1967, and 1968. Denver 12 MDT.

TABLE 4.

Mean wind shear magnitudes for hail intensity categories.

Category	Mean Shear sfc-500 mb	Mean Shear 500 mb-250 mb	Comparison with Ratner 500 mb-250 mb
heavy hail	35 kts	29 kts	All
standard deviation kts	13	13	Hail Days
moderate hail	33	27	22 kts
standard deviation	12	11	
light hail	26	31	All No
standard deviation	9	14	Hail Days
no hail echoes	23	31	30 kts
standard deviation	10	18	
no hail-no echoes	24	31	
standard deviation	11	14	

Presentation of Mean Radar Echo and Storm Motion

The observations of radar echo and storm motions were stratified into hail intensity categories. The observations in each category were then averaged to produce mean values of radar echo and hailswath speed and direction. The results are presented in Table 5. Also presented, for comparison, are the corresponding mean environmental winds at 600 and 500 mb; the levels which best match the mean radar echo motions. The mean environmental winds presented correspond to days on which radar echo motions were measured, and are not mean winds for the entire hail season.

Newton's Hypothesized Mechanism of Hydrodynamically Induced Cloud Development

Newton (1959) assumed that a large cloud mass could be approximated by a rigid cylinder. He hypothesized that the cylinder would travel in a sheared wind field with a mean velocity which was faster than the lower level winds, and slower than the upper level winds. Newton considered that vertical transport of conserved horizontal momenta of the winds by the circulation systems of a large cloud mass produced a homogenous momentum within the cloud. This caused the cloud to move at all levels with approximately the same velocity.

TABLE 5.

Summary and comparison of mean hailswath onset progression
rate, mean radar echo motion, and corresponding mean
environmental wind data measured during the summer of 1967.

Categories	hailswath mean		radar echo mean		environmental wind 600 mb (mean) 500 mb			
	dir	speed	dir	speed	dir	speed	dir	speed
	deg	kts	deg	kts	deg	kts	deg	kts
heavy hail standard deviation-kts	290 (6 cases)	25 8	280 (12 cases)	24 8	270	18	260	31
moderate hail standard deviation-kts	--	--	300 (5 cases)	24 6	290	15	280	30
light hail standard deviation-kts	--	--	300 (6 cases)	15 7	280	17	290	15
no hail-echoes standard deviation-kts	-	-	300 (8 cases)	14 3	360	13	300	13

Environmental air possessing the horizontal momentum of the
mid-level winds is thought to be incorporated into the downdraft by
the action of precipitation falling into clear air from the upper
levels of the cloud. Chilling of the usually drier environmental air
by the evaporation of precipitation produces negative buoyancy and
sinking (Ludlam, 1963). Thus a greater amount of horizontal momentum
is incorporated into the downdraft than could be imparted to it by the
impingement of the environment at lower levels. The existence of a
vigorous, horizontally moving downdraft is essential to Newton's
hypothesis.

Environmental air possessing the horizontal momentum of the
low level winds is thought to be transported by the updraft to the
upper regions of the cloud, where it tends to oppose the motion of
the environment. Thus interchange of lower and higher level kinetic
energies of the environment within the cloud, along with turbulent
mixing of these energies, tends to resist the effect of the shearing
force of the wind field on the cloud mass.

Hitschfeld (1960) discussed radar observations of well-developed thunderstorms which remained upright in the presence of severe wind shear of the order of 100 knots from the base to the top of the cloud. He pointed out that "the rapid vertical motions within the storm give it a semblance of rigidity," with rising parcels passing through the levels of high winds in as little as several minutes. The data of Hitschfeld indicated that the echoes moved at all levels with the same velocity. This velocity was roughly that of the lower wind between 7 -- 10 kft.

Figure 5 after Newton (1959), shows how non-hydrostatic pressures are developed due to the wind shear in the case of wind shear with no directional veering. In Figure 5, the cloud is moving with mean velocity V_c. The lower portion of the cloud is overtaking the slower environmental winds. while at the upper portion of the cloud, the environmental winds are overtaking the slower moving cloud top. The non-hydrostatic pressure excesses and deficits, shown as pluses and minuses, are functions of the squares of the relative wind velocities. Relative wind streamlines are shown to indicate the direction of relative flow and the respective locations of the stagnation, or impingement, points on the cylinder. Flow-induced effects on the flanks of the cylinder have been neglected to simplify illustration of the concept. The rigid cylinder, which is used to approximate the cloud, extends from the cloud top to the earth's surface in order to include the subcloud updraft-downdraft region.

For the case of wind shear with directional veering, Newton employed an empirically derived dynamic pressure distribution around the cylinder similar to that presented in Goldstein (1938). This permitted determination of the non-hydrostatic pressure at points located directly above the near-surface stagnation point in order to compute the vertical gradient of non-hydrostatic pressures. Figure 6 shows the typical distribution of flow-induced non-hydrostatic pressure coefficients on the cylindrical cloud mass due to veering of the relative wind. The pressure coefficients K are taken from Figure 8 of Newton (1959). The pressure coefficient K relates the stagnation point pressure (K = +1.0) to the non-hydrostatic pressure at any
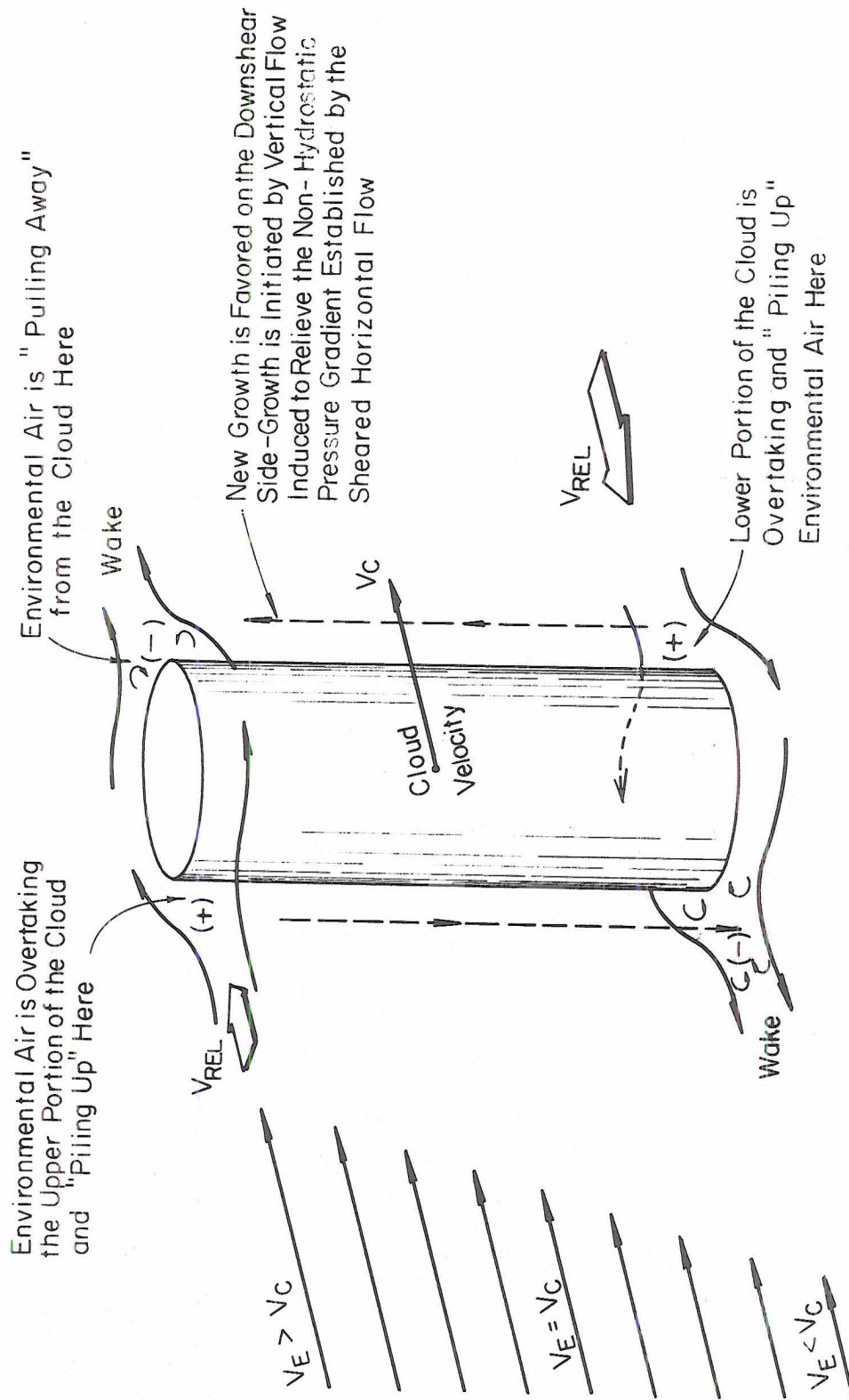
Figure 5. The effect of the flow around a cloud mass in a sheared wind field with no directional veering. After Newton (1959).
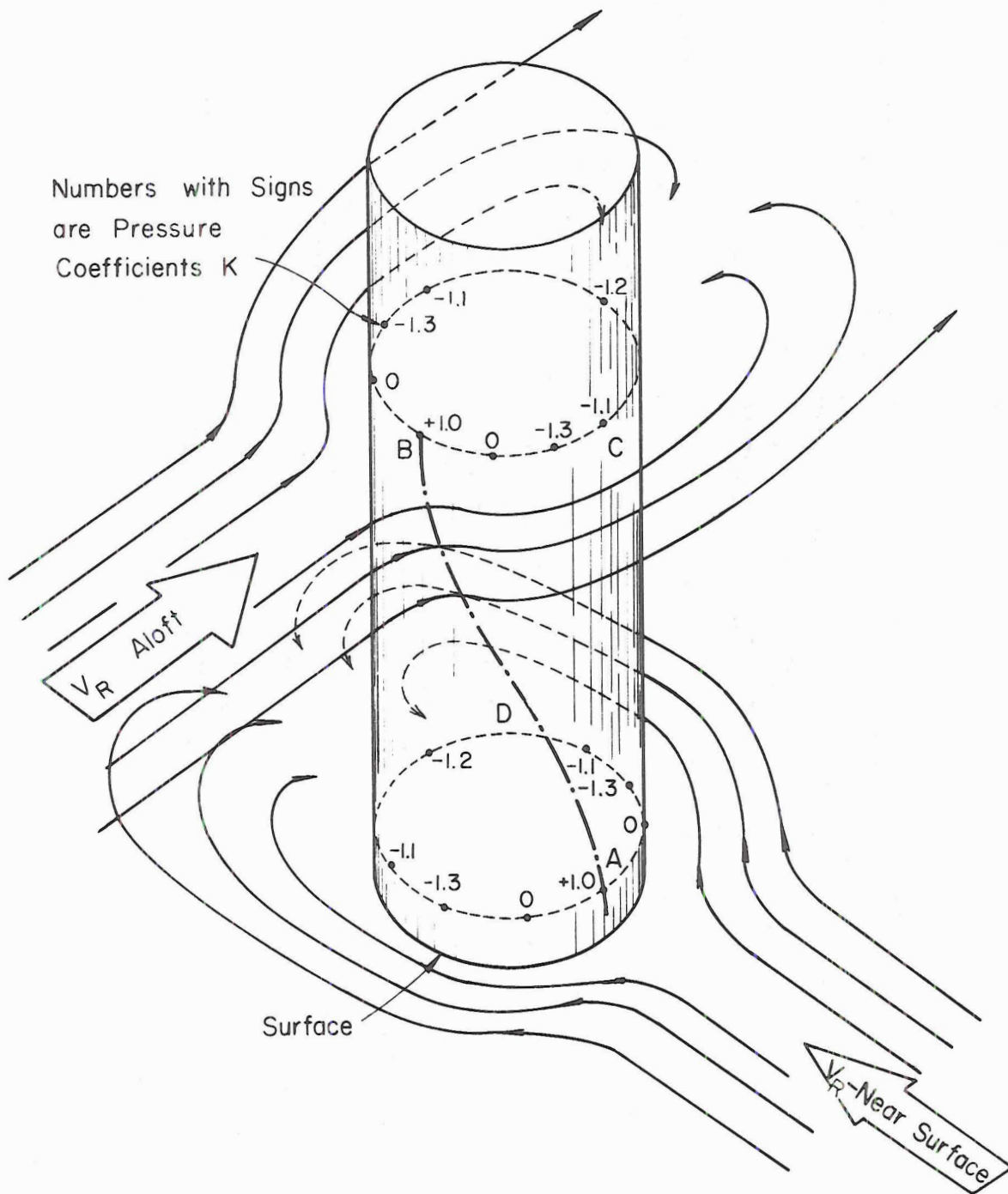
Figure 6. Typical distribution of flow-induced pressure
coefficients on a cloud mass due to veering
of the relative wind. After Newton (1959).

point around the circumference of the cylinder at a given level.
Point "C", located directly above the near-surface flow stagnation
point "A", has a negative pressure coefficient due to its location
in the flow path around the cylinder at that level.

The vertical gradient of the non-hydrostatic, or hydrodynamic,
pressure is taken along line A-C. A reduction of non-hydrostatic
pressure with height induces an upward directed acceleration of the
impinging near-surface relative wind flow. Curved line A-B on the
surface of the cylinder is the locus of stagnation points with height
due to the veering of the relative wind between the two levels. Figure
7 shows the characteristic veering of the relative wind around a cloud
mass whose motion was measured by a CSU M-33 research radar located at
Ault, Colorado, on July 25, 1967. The relative wind is the vector
difference between the environmental wind at each level and the radar
echo motion.

The magnitude of the non-hydrostatic pressure at any level and
at any location on the periphery of the cylinder is determined by
multiplying the stagnation pressure, which is the same as the kinetic
energy per unit volume, $1/2\rho V_R^2$, by the corresponding pressure coef-
ficient K. The non-hydrostatic, or hydrodynamic, pressure is
designated by the symbol H, i.e., $H = K \, 1/2\rho V_R^2$.

The pressure coefficients were determined at a Reynolds number,
$R_e = \rho V_R D/\mu$, of 3×10^4. This corresponds to $V_R = 10$ mps, $D = 30$ km
dia., $\mu = 100$ gm.cm^{-1} sec^{-1}, and ρ 10^{-3} gm.cm^{-3}, the values used by
Newton in the 1959 analysis.

In the present analysis only the vertical gradients of non-
hydrostatic pressure were considered. Horizontal gradients of non-
hydrostatic pressure were present, and the forces produced by them
tended to shear the cloud downwind. Newton (1959) showed that
smaller cumulus clouds lack the internal structures of strongly
developed downdrafts and rapid updrafts required to oppose the
shearing forces of their wind environments. Aspects of the marked
sloping of sheared cumuli have been treated in detail by Malkus
(1949), and Byers and Battan (1949).

255°

25 mps

16 mps

240°

9 mps

245°

8 mps

255°

5 mps

235°

160°

6 mps

135°

6mps

145°

6mps

200 mb

300 mb

400 mb

The Cloud Mass is
Represented by Cylinder

500 mb

600 mb

The Cloud Velocity is
8 mps from 330°

700 mb

800 mb

SFC

The Arrows
Represent
Horizontal Wind
Flow
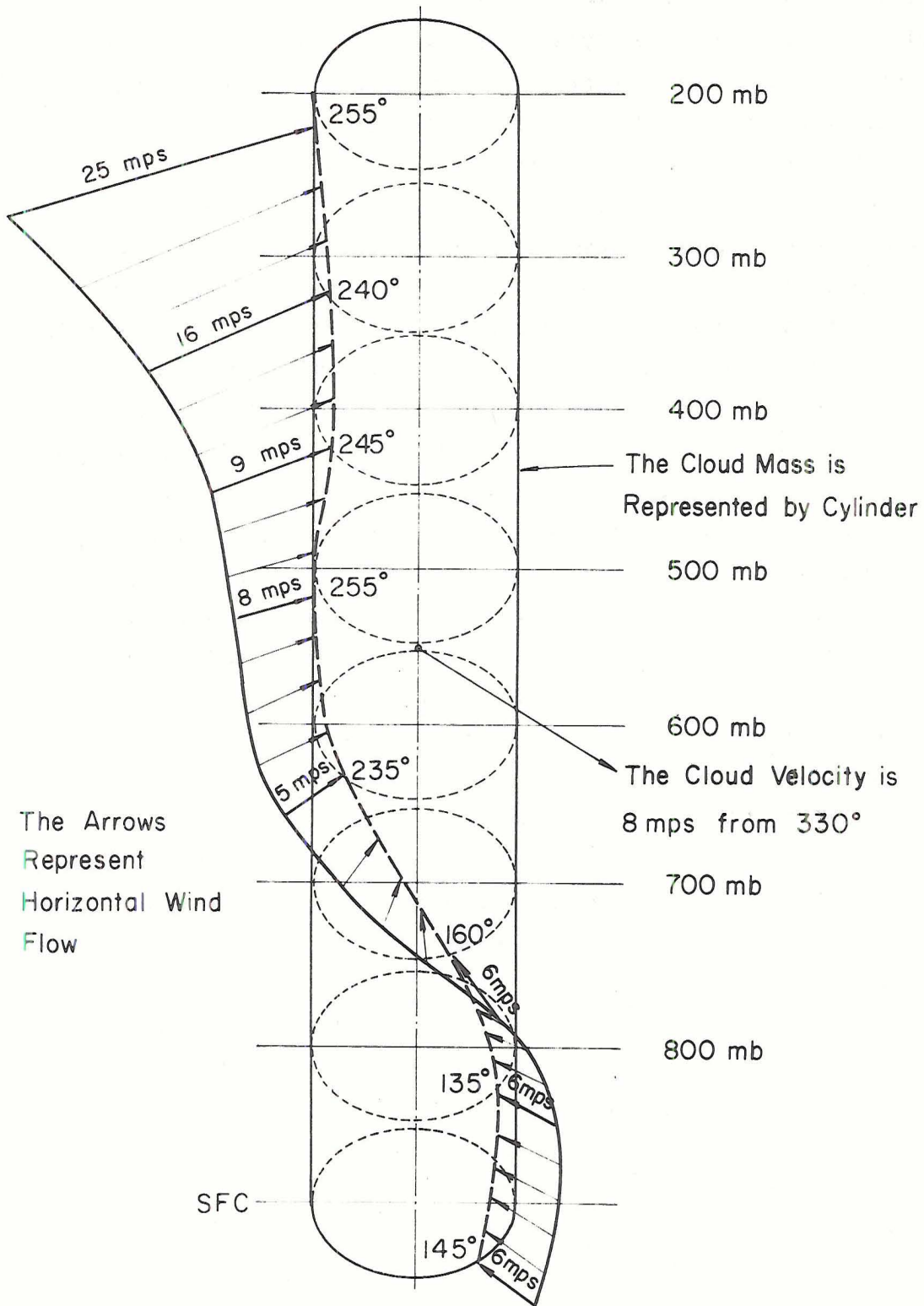
Figure 7.   Actual distribution of the relative wind velocity
V_R around a cloud mass on 25 July 1967.

In order to derive a quantitative means of expressing the fore-going, and applying it to the conditions of Northeastern Colorado, we begin with the vertical equation of motion

$$\frac{dw}{dt} = - \frac{1}{\rho_a} \frac{\partial P}{\partial Z} - g, \tag{1}$$

where ρ_a is the density of the air column being accelerated.

Following Newton (1959), the total pressure p of the air column at a given level is composed of a hydrostatic component p_h, and a hydrodynamic component H:

$$p = p_h + H. \tag{2}$$

Substituting (2) into the equation of motion yields

$$\frac{dw}{dt} = - \frac{1}{\rho_a} \left(\frac{\partial P_h}{\partial Z} + \frac{\partial H}{\partial Z}\right) - g. \tag{3}$$

If the environment surrounding the column of air is assumed to be in hydrostatic balance, and if pressure coordinates are substituted in the right-hand side of (3), we have:

$$\frac{dw}{dt} = g\left(\frac{\rho_e}{\rho_a} - 1\right) + g \frac{\rho_e}{\rho_a} \frac{\partial H}{\partial P_h}. \tag{4}$$

Using the equation of state to express the ratio $\frac{\rho_e}{\rho}$ in terms of pressure and temperature of the undisturbed environment, and of the column of air being accelerated, the following density ratio can be defined:

$$\frac{\rho_e}{\rho_a} = \frac{Pe}{P} \frac{T}{T_e}. \tag{5}$$

The temperature T of the updraft column is composed of an environmental temperature T_e, and a difference over the environmental temperature of ΔT:

$$T = T_e + \Delta T. \tag{6}$$

The effect of moisture, except for the pseudo-adiabatic process within the cloud, is not taken into account in this analysis.

The hydrostatic pressure p_h is considered to be the same as the environmental pressure p_e, therefore from (2):

$$p_h = p - H = p_e. \tag{7}$$

The substitution of (6) and (7) into (5) gives

$$\frac{\rho_e}{\rho} = (1 - \frac{H}{P})(1 + \frac{\Delta T}{T_e}). \tag{8}$$

Substituting (8) into (4) yields,

$$\frac{dw}{dt} = g[(1 - \frac{H}{P})(1 + \frac{\Delta T}{T_e}) - 1] + g[(1 - \frac{H}{P})(1 + \frac{\Delta T}{T_e})\frac{\partial H}{\partial P_e}], \tag{9}$$

or upon rearrangement:

$$\frac{dw}{dt} = g[\frac{\Delta T}{T_e} - \frac{H}{P} - \frac{H}{P}\frac{\Delta T}{T_e} + \frac{\partial H}{\partial P_e} + \frac{\partial H}{\partial P_e}\frac{\Delta T}{T_e} - \frac{\partial H}{\partial P_e}\frac{H}{P} - \frac{\partial H}{\partial P_e}\frac{H}{P}\frac{\Delta T}{T_e}]. \tag{10}$$

Examination of the terms within the brackets revealed that their relative magnitudes varied considerably. Substitution of typical atmospheric measurements into the terms permitted the following comparisons:

First term: $\frac{\Delta T}{T_e}$:

ΔT = 1 degree K departure from the environment (horizontal gradient);

T_e = 260 degrees K environment temperature (mean layer temperature)

$\frac{\Delta T}{T_e} = \underline{39 \times 10^{-4}}$.

at $T_e = 213°K$; $\frac{\Delta T}{T_e} = \underline{47 \times 10^{-4}}$.

Second term: $\frac{H}{P} = 1/2\rho V_R^2/p$; evaluated for near the surface and again for near the tropopause.

Near the surface:

$p = 800$ mb $= 8 \times 10^5$ gm.cm^{-1} sec^{-2}

$\rho = 1 \times 10^{-3}$ gm.cm^{-3}

$V_R = 20$ mps; $V_R^2 = 4 \times 10^6$ cm^2 sec^{-2}

$\frac{H}{P} = 1/2 (1 \times 10^{-3}$ gm.cm$^{-3})(4 \times 10^6$ cm^2 sec$^{-2})/8 \times 10^5$ gm.cm^{-1} sec^{-2} = $\underline{25 \times 10^{-4}}$

Near the tropopause:

$p = 200$ mb $= 2 \times 10^5$ gm.cm^{-1} sec^{-2}

$\rho = .32 \times 10^{-3}$ gm.cm^{-3}

$V_R = 20$ mps

$$\frac{H}{P} = 1/2(.32 \times 10^{-3} \text{ gm.cm}^{-3})(4 \times 10^6 \text{ cm}^2 \text{ sec}^{-2})/2 \times 10^5 \text{ gm.cm}^{-1} \text{ sec}^{-2} =$$

$$32 \times 10^{-4}$$

Third term: $\quad \frac{H}{p}\frac{\Delta T}{T_e} = (.0025)(.0039) = \underline{0.098 \times 10^{-4}}$

Fourth term: $\quad \frac{\partial H}{\partial p_e}$ evaluated for near the surface, and near the

tropopause.

Near the surface:

$p = 800$ mb, $V_R = 20$ mps

$p = 700$ mb, $V_R = 10$ mps

$H_{800} = 2.0$ mbs

$H_{700} = 0.5$ mbs

$$\frac{\partial H}{\partial p_e} = \frac{1.5 \text{ mb}}{100 \text{ mb}} = \underline{150 \times 10^{-4}}$$

Near the tropopause:

$p = 300$ mb, $V_R = 10$ mps

$p = 200$ mb, $V_R = 20$ mps

$H_{300} = 0.23$ mb

$H_{200} = 0.64$ mb

$$\frac{\partial H}{\partial p_e} = \underline{41 \times 10^{-4}}$$

Fifth term: at 800 mb—

$$\frac{\partial H}{\partial p_e}\frac{\Delta T}{T_e} = (.015)(.0039) = \underline{0.59 \times 10^{-4}}$$

Sixth term: at 800 mb—

$$\frac{\partial H}{\partial p_e}\frac{H}{p} = (0.015)(0.0025) = \underline{3.8 \times 10^{-4}}$$

Seventh term: at 800 mb—

$$\frac{\partial H}{\partial p_e}\frac{H}{p}\frac{\Delta T}{T_e} = (.015)(.0025)(.0039) = \underline{0.0015 \times 10^{-4}}$$

Terms one, two, and four may therefore be treated without concern for the remaining terms, which have been shown to be at least one order of magnitude smaller. This offers numerical confirmation of a similar conclusion reached by Newton. In addition, Newton considered term two to be negligible for the purposes of his analysis. The foregoing comparisons, summarized in Table 6, have shown that term two is typically negligible at the lower levels, compared with term four. In the upper half of the troposphere, however, term two can be of the same order of magnitude as terms four and one. Term two is therefore retained in the analysis.

It should be noted that the assumption of $\Delta T = 1C$ in the evaluation of term one is conservative. For the updraft core of a well established cumulonimbus capable of acting as an obstacle to the environmental wind, $\Delta T = 3$ to $6C$ may be more representative of actual conditions. Sulakvelidze (1965) cites a mean ΔT of $5C$, with values ranging from 2 to $9C$, for a sampling of hailstorms in the Caucasus.

Equation (10) may now be written as

$$\frac{dw}{dt} = g\left(\frac{\Delta T}{T_e} - \frac{H}{P} + \frac{\partial H}{\partial P_e}\right), \qquad (11)$$

where the first term describes the contribution to vertical acceleration from the thermal buoyancy, and the remaining terms describe the contribution due to the hydrodynamic interaction of the cloud with the environmental wind. The third term is so defined that a reduction of the non-hydrostatic pressure excess with increase in height, or an increasingly negative non-hydrostatic pressure deficit with increase in height, yields a positive, upward directed acceleration.

The second term on the right-hand side of (11) represents the ratio between the induced hydrodynamic (non-hydrostatic) pressure in the air column being accelerated, and the total pressure; i.e., the hydrodynamic plus the hydrostatic, within the column. The second term arises in the derivation of equation (11) because of the expansion of $\frac{\partial P}{\partial Z}$ into hydrostatic and hydrodynamic components. This

TABLE 6.

Summary of the order of magnitude evaluation of equation (10).

terms within the brackets of eq. (10)		near the surface	near the tropopause
one -	$\dfrac{\Delta T}{T_e}$	39×10^{-4}	47×10^{-4}
two -	$\dfrac{H}{p}$	25×10^{-4}	32×10^{-4}
three -	$\dfrac{H}{p}\dfrac{\Delta T}{T_e}$	0.098×10^{-4}	1.15×10^{-4}
four -	$\dfrac{\partial H}{\partial P_e}$	150×10^{-4}	41×10^{-4}
five -	$\dfrac{\partial H}{\partial P_e}\dfrac{\Delta T}{T_e}$	0.59×10^{-4}	0.19×10^{-4}
six -	$\dfrac{\partial H}{\partial P_e}\dfrac{H}{p}$	3.8×10^{-4}	1.13×10^{-4}
seven -	$\dfrac{\partial H}{\partial P_e}\dfrac{H}{p}\dfrac{\Delta T}{T_e}$	0.0015×10^{-4}	0.00062×10^{-4}

expansion has the effect of rendering the vertical acceleration $\dfrac{dw}{dt}$ dependent on the horizontal wind velocity as well as the static pressure and temperature.

It was found convenient to establish the following symbols for the terms of equation (11):

$$g\,\frac{\Delta T}{T_e} = A_t \tag{12}$$

$$g\,\frac{H}{p} = A_n \tag{13}$$

$$g\,\frac{\partial H}{\partial P_e} = A_H \tag{14}$$

The term A_n, usually much smaller than A_H', subtracts from the positive, upward directed acceleration at the lower levels, according to the sign of the second term in the right-hand side of (11). At the higher levels, however, this term becomes additive. This is due to a sign change of H. The negative sign is associated with the negative pressure coefficient (-K) introduced by the usual marked veering of the relative winds with height about a moving storm.

It should be again emphasized that a major effect of marked vertical wind shear is to position aloft a hydrodynamic pressure deficit (-H) directly above a hydrodynamic pressure excess (+H) near the surface. This markedly increases the magnitude of the gradient in (14).

For computational purposes, (13) and (14) were lumped together into an acceleration factor termed A_H. This term accounted for the full effect of the wind shear induced contribution to cloud development and structure.

The acceleration factor A_H was computed for each 100 mb layer from the surface to the 300 mb level, and for each 50 mb layer above that level to the top of the cloud. This computation was performed for 20 days of the 1967 hail season.

It should be noted that the effect of the downdraft diverging at the surface was included in the determination of the near-surface relative wind, V_R, for each of the 20 cases of 1967. Following Newton (1959), an assumed 10 mps outflow velocity was added to the near-surface relative wind for each case. For a cylindrical downdraft of 3 km radius and a 500 m outflow depth, this assumed outflow velocity is equivalent to a downdraft velocity of 3.4 mps. This compares with a mean downdraft velocity of 7.1 mps for downdrafts associated with reports of hail in Ohio. These measurements, taken from Byers and Braham (1949), apply to the layer between 5,000 and 10,000 feet.

Parcel Theory of Thermal Buoyancy

The first term of equation (11) is identical to the expression given for the well-known parcel theory of buoyancy. The parcel

theory expression is derived in an analogous manner to equation (11), but without expanding the pressure gradient term of the vertical equation of motion into static and dynamic components. Equation (11) degenerates into the simple temperature dependent parcel theory expression upon the assumption of $V_R = 0$, which implies $H = 0$, thus eliminating the second and third terms.

Parcel theory tends to over-estimate the vertical velocities and cloud top heights actually achieved by smaller cumuli. This is ordinarily credited to the neglect of the entrainment of dry environmental air, and to the neglect of the resistive forces of form and frictional drag. The entrainment of dry environmental air will evaporate condensed moisture, and, through cooling, reduce the buoyancy of the updraft.

Parcel theory is believed to apply more realistically to updrafts of the very largest storm masses (Malkus, 1960; Ludlam, 1963). The larger diameter updrafts have a reduced percentage of surface area to volume compared to smaller updrafts. This has the effect of diminishing the factor of entrainment and mixing through the cloud surface for the larger clouds. Newton (1966) offered the explanation that "the cores of updrafts are considered to be essentially unmixed, while their outersheaths undergo strong mixing with the environment." Ludlam (1966) pointed out that the environments are often the nearly-saturated residues of earlier updrafts. This factor further reduces the effect of entrainment and mixing.

The assumption of a continuous plume updraft eliminates the possibility of wake entrainment, i.e., entrainment into the base of a rising updraft element, or bubble. This form of entrainment is due to the return flow of the displaced environmental air into the wake of a rising bubble, where it is incorporated into the ring vortex-like internal circulation of the bubble. This mechanism has been treated in detail by Scorer and Ludlam, (1953), and Levine (1959).

The analysis presented in this paper considers only the protected cores of the largest updrafts. It is here that the maximum horizontal

temperature differences, and consequently the highest achievable vertical velocities are expected to exist.

Temperature soundings taken on the 20 case days of 1967 were analyzed for mean values of ΔT, and T_e, for each 100 mb layer from the cloud base to the 300 mb level, and for each 50 mb layer above 300 mb to the cloud top. The value ΔT was measured from the difference between the sounding temperature and the appropriate moist adiabat. The cloud base height and the appropriate moist adiabat were determined by lifting the surface dew point along the corresponding moisture isopleth until the sounding temperature curve was intersected. The acceleration factor a_T was then computed by substitution of the fore-going quantities into equation (19).

While and analysis of this paper considers only the protected cores of the updrafts, it was of interest to show the effect of assumed entrainment on an updraft. The five no hail-echoes soundings from the 20 case days of 1967 were re-evaluated, considering entrain-ment at a rate of 100 percent in 300 mbs. The entrainment rate chosen was in the middle of the range of rates cited by Byers and Braham (1949) for thunderstorms in Florida and Ohio, and by Stommel (1947) for trade cumuli. The modified acceleration factor was designated a_T'. The graphical procedure described by Austin (1948) was employed to modify the soundings. An example of the application of this procedure is given by Byers (1959).

Derivation of Rainstorm and Hailstorm Vertical Velocity Profiles

The vertical acceleration factors, a_T, a_H, and a_C, where $a_C = a_T + a_H$, were each integrated incrementally to yield profiles of vertical velocity. The profiles are presented in Figs. 8 through 10. The expression used for the incremental integration,

$$V_2{}^2 = V_1{}^2 + 2a(Z_2 - Z_1),\tag{15}$$

is well known from Physics and describes the velocity changes of a freely-moving particle in rectilinear motion under the influence of
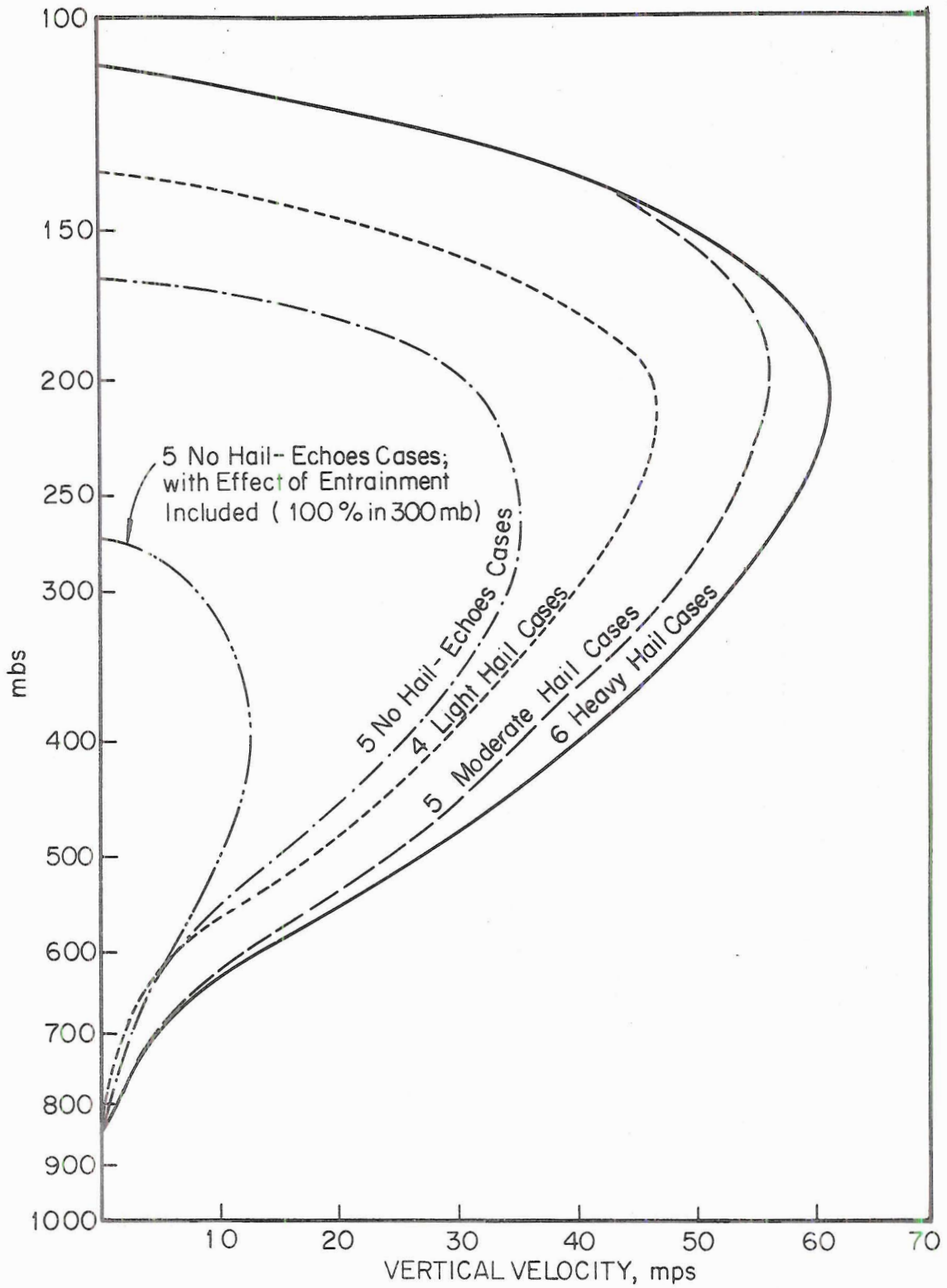
Figure 8. Mean profiles of vertical velocity due to thermal
instability alone. These profiles were derived
from 20 cases observed during the summer of 1967.
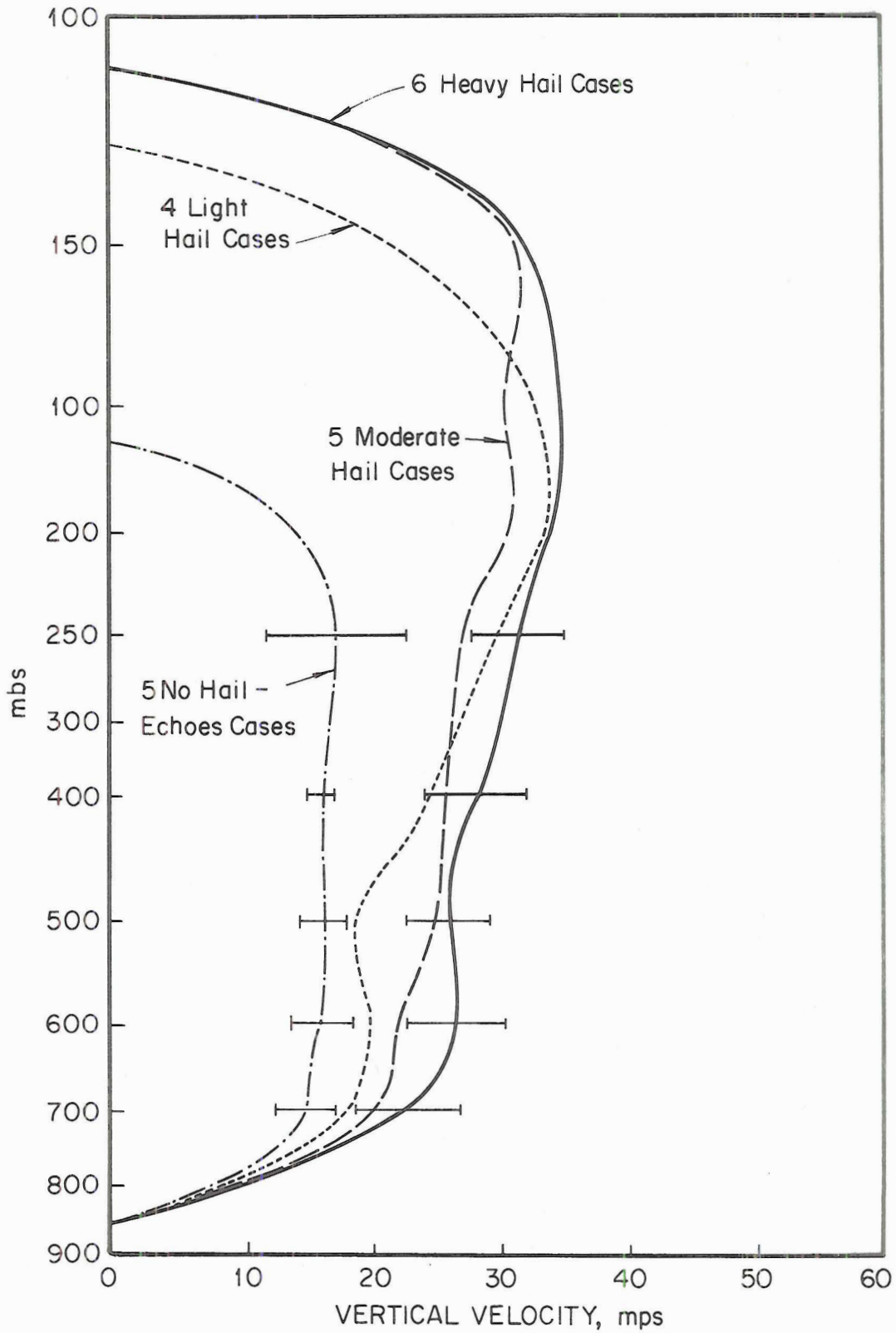
Figure 9. Mean profiles of vertical velocity due to the
hydrodynamic interaction between storm and
environmental wind considered alone. These
profiles were derived from the 20 cases of 1967.
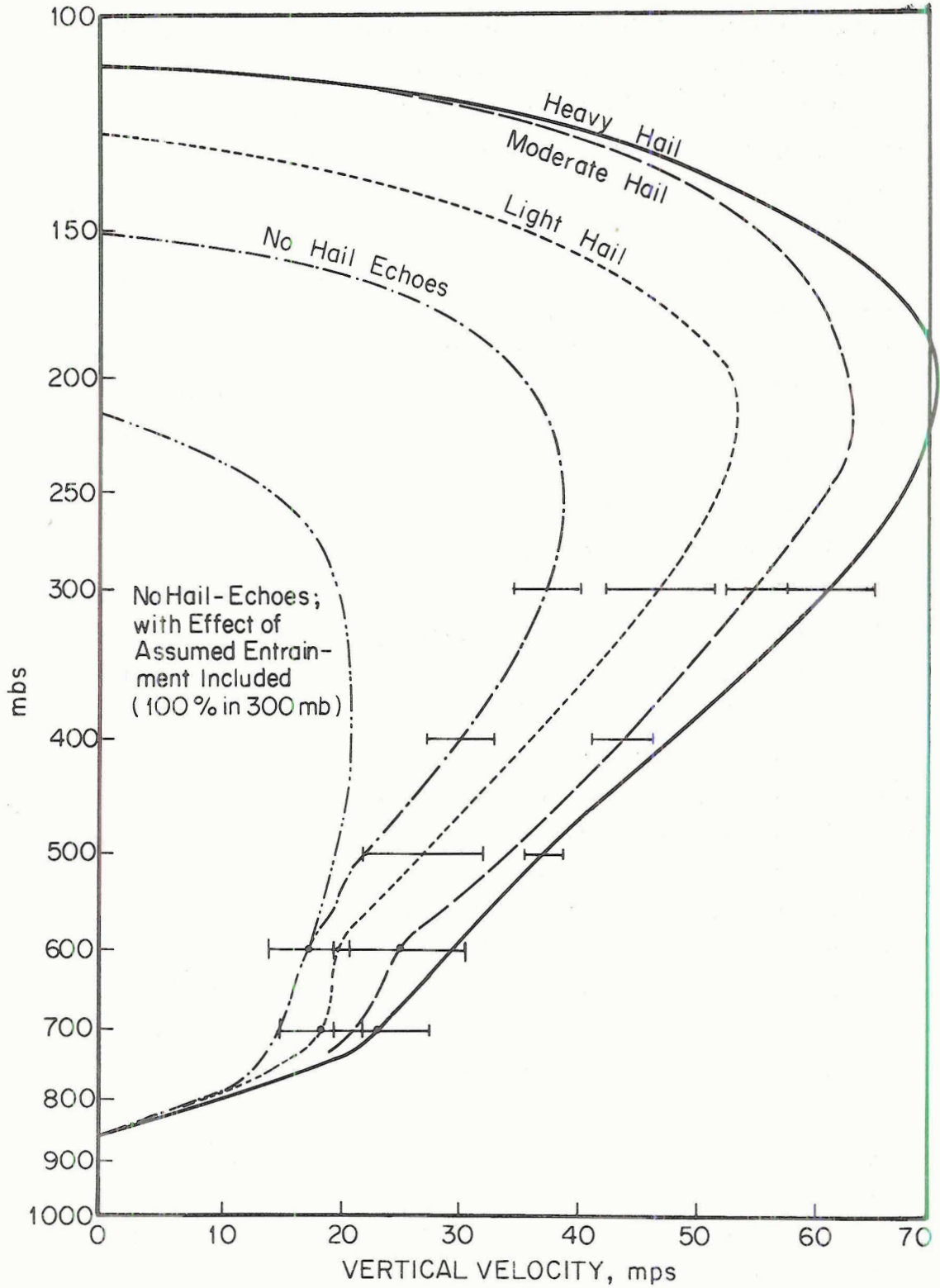
Figure 10. Mean profiles of cloud total vertical velocity
due to the combined effect of thermal and hydro-
dynamic instability. These profiles were derived
from 20 cases observed during the summer of 1967.
The range of one standard deviation is shown.

an accelerating force. The symbols Z_1 and Z_2 are the limits-of-integration boundary heights. The limits of each successive integration were defined by layers of 100 mb thickness near the top of the cloud. The heights used were those of the standard atmosphere. The acceleration factor, a, which was computed for the midpoint of each layer, was assumed to be constant throughout the layer.

The integration of a_T, the thermally induced acceleration factor, was begun at cloud base with an initial velocity of 5 mps. This was a typical vertical velocity at cloud base measured during CSU updraft studies. The integration of a_H, the hydrodynamically induced acceleration factor, was begun from the surface with no initial vertical velocity.

The cloud top was defined to be the level at which the vertical velocity became zero, neglecting any overshoot and subsequent oscillation of the updraft. Above the tropopause the factor a_T is generally negative and large in magnitude compared to a_H. The factor a_T, therefore, essentially determines the height of the cloud top.

The Effect of Precipitation Accumulation on Updraft Strength

The effect of the water condensed during the ascent of a particular parcel of updraft has been neglected. The accumulation of precipitation particles formed aloft during previous updraft ascents, however, may have a significant effect on subsequent updrafts.

In order to determine the effect of the accumulation of precipitation on updraft strength, several reasonable concentrations of raindrops and hailstones were superimposed on a previously derived updraft vertical velocity profile. The assumption was made that the largest particles were located between 400 and 500 mb. This height is in agreement with profiles of radar reflectivity with height, which provide evidence of the presence of large particles (Atlas, 1963). Location of a reflectivity maximum at this height is in broad agreement with the findings of Donaldson (1962), Sulakvelidze (1965) and Fischer.[1] It was further assumed that the updraft

---

[1]Fischer, R. E., Colorado State University, 1968, personal communication.

streamed through the precipitation accumulation zone, expending some
of its momentum to suspend each particle encountered. In actuality,
the first particles encountered are probably elevated. As the
updraft is decelerated higher particles encountered settle, tending
to concentrate the particles into a blanket of rather shallow depth.
The precipitation particle accumulation is thus located immediately
above an updraft velocity maximum. This process has been described
in detail by Marshall (1961), Sulakvelidze (1965), and Irabarne
(1968).

Deceleration of the updraft is accompanied by its divergence. In
this analysis, the only effect of updraft divergence is to change the
angle of impingement on the suspended precipitation particles. Greater
divergence would therefore reduce the vertical component of updraft
velocity. At an impingement angle of 45 degrees, the vertical com-
ponent would still be as much as 71 percent of the diverged air
velocity. The error due to omitting the effect of updraft divergence,
therefore, becomes important only for great reductions of updraft
velocity.

The aerodynamic drag on the precipitation particles impart a
retarding force to the rising updraft in accordance with the following
relationship:

$$F = NA \ C_D \ 1/2 \ \rho_A V_T^2, \tag{16}$$

where V_T is the terminal velocity of the particle, or the velocity of
the particle with respect to the updraft, ρ_A is the density of the
updraft at 450 mb, C_D is a drag coefficient for the flow of the
updraft around the precipitation particles, A is the cross sectional
area of each particle, and N is the number of particles in the volume
streamed through by a unit mass of updraft. The particle size dis-
tribution spectrum is assumed to be monodisperse.

The deceleration A_p offered by the retarding force F acting on
the unit mass m of updraft, per second, is

$$\frac{F}{M} = A_p \tag{17}$$

The factor A_p thus derived was combined with the accelerating factors A_T and A_H;

$$A_C' = A_T + A_H - A_p. \qquad (18)$$

The acceleration factor A_C' applied only to the 500-400 mb layer.

The deceleration factor A_p was determined for a range of particle sizes and concentrations at the conditions existing at 450 mb. Table 7 summarizes the results of this computation.

TABLE 7.

Values of A_p for a range of particle sizes and water contents.

diameter d	terminal velocity V_T	C_D	water content gm. M^{-3}				
			1	5	10	25	50
rain:			A_p = cm.sec^{-2}				
1 mm	4.0 mps	.67	0.80	4.0	8.0	20	40
2	6.5	.52	0.82	4.1	8.2	21	41
3	8.1	.50	0.80	4.0	8.0	20	40
4	8.8	.56	0.81	4.0	8.1	20	40
5	9.1	.66	0.82	4.1	8.2	21	41
			hail concentrations				
			.01 stones M^{-3}	1 stone M^{-3}		30 stones M^{-3}	
hail: 2 cm	25.0 mps	.50		2.5 cm.sec^{-2}		74.1 cm.sec^{-2}	
5	39.0	.50	0.8 cm.sec^{-2}				

The value of the air density selected for 450 mb was 0.58×10^{-3} gm.cm^{-3} (-10C). The raindrop terminal velocities were from Gunn and Kinzer (1949), and the raindrop drag coefficients were abstracted from List (1949). The drag coefficients for the hailstones were from Fig. 1 of List (1961).

Hailstone drag coefficients can range from 0.45 for smooth
spheres, to 0.8 for ellipsoidal shapes, according to Ludlam and
Macklin (1961). Willis (1964), measured a drag coefficient of
0.24 for a roughened, large, dry free-falling ice sphere. The
Reynolds Number was supercritical during this measurement. Willis
showed that drag coefficients could double when the falling stones
began melting. He cited the transition from turbulent flow to the
laminar flow regime as the cause of the drag coefficient increase.

Bilham and Relf (1937) measured a drag coefficient $K_d = 0.24$,
for spheres towed by an aircraft. The two authors used the symbol
K_d in place of $1/2C_D$. Their drag coefficients, therefore, should
be multiplied by two for comparison with the drag coefficients
presented by, for example, Goldstein (1938), or Hoerner (1958).
For the present analysis it was assumed that the hail would be wet
and smooth-textured, with a C_D of 0.5.

Figure 11 shows the effect of variation of C_D on hailstone
terminal velocity. The terminal velocity is reached when the
weight of the hailstone equals the aerodynamic drag upon it.
Then the velocity of the hailstone with respect to the air remains
constant. The expression for the terminal velocity of the hail-
stone is

$$V_T = (\frac{4}{3} \frac{\rho_i \, d \, g}{\rho_a \, C_D})^{1/2} \tag{19}$$

where d is the hailstone diameter, g is the acceleration of gravity,
and ρ_i is the hailstone density. Figure 11 was based on this
expression. The terminal velocities for the hailstones in Table 7
were taken from Figure 11.

In order to show the effect of the derived deceleration factors
on a typical, heavy hail vertical velocity profile, A_p factors for
several concentrations of 2 and 5 mm diameter raindrops, and 2 and 5 cm
diameter hailstones were substituted into equations (18) and (15).
Equation (15) was integrated incrementally from 400 mb upward to
modify the profile. The results of this procedure are shown in
Figure 12.
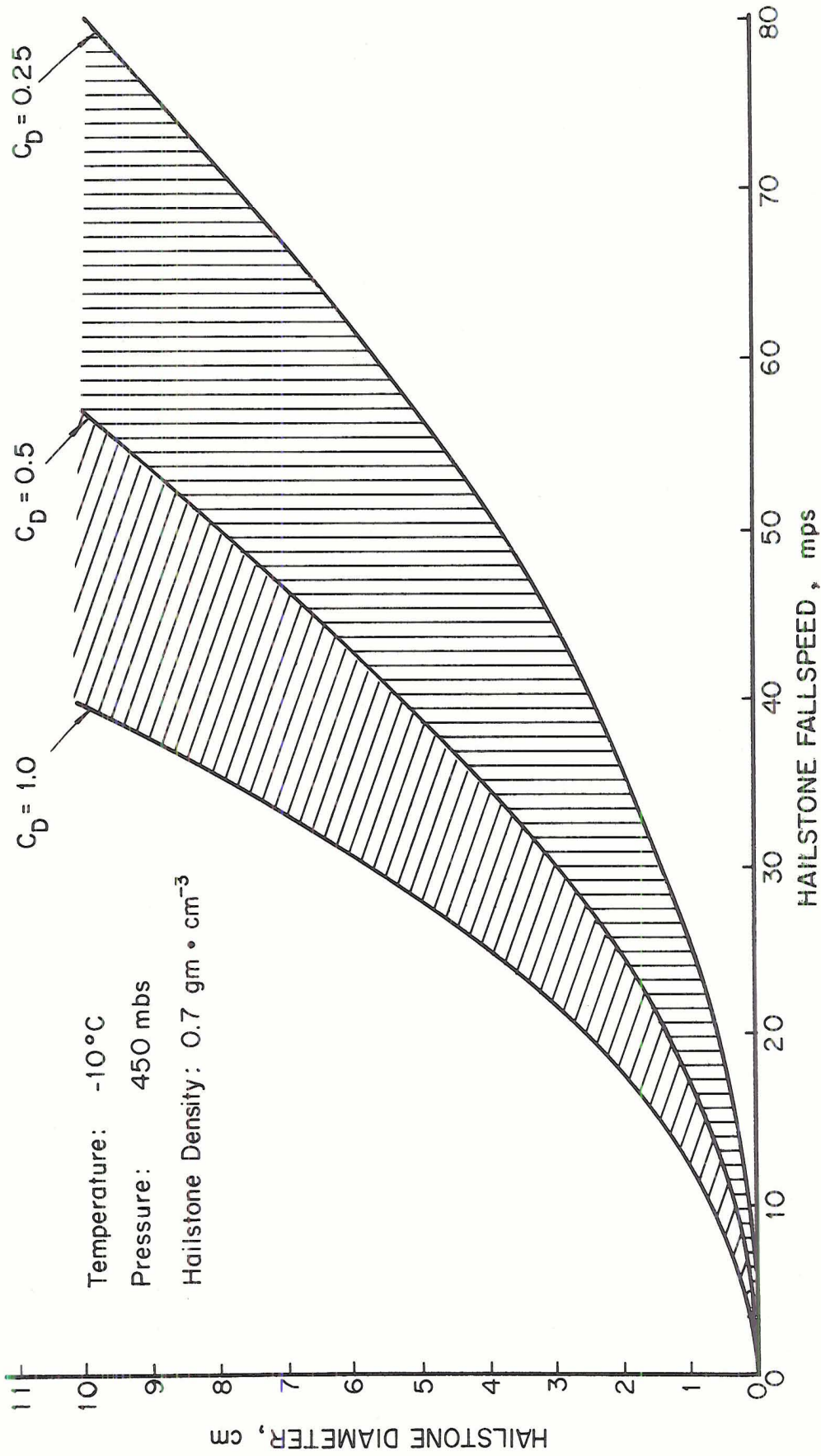
Figure 11. The effect of the variation of C_D on hailstone terminal velocity.
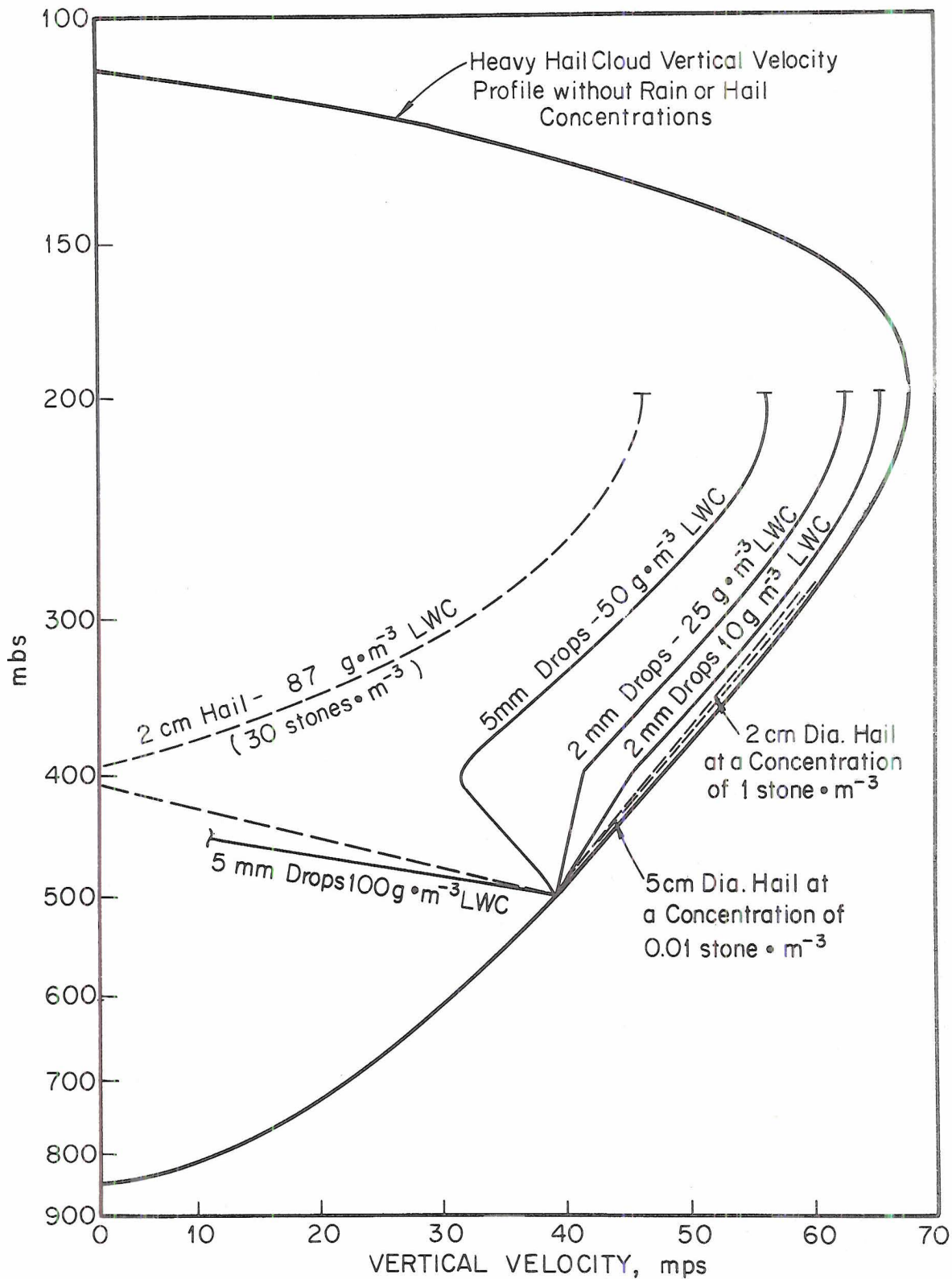
Figure 12: The effect of imposed rain and hail accumulations on a cloud vertical velocity profile.

III. DISCUSSION OF RESULTS

Mean Windspeed Profiles for Northeastern Colorado

The mean windspeed profiles for the hail seasons of 1966, 1967, and 1968 are shown in Fig. 3. This comparison shows the relative windspeeds aloft for varying categories of hail intensity. The presence of higher mean windspeeds with increasing hail intensity is clearly shown.

The physical implication of the gradation of these profiles is that correspondingly greater kinetic energy was available aloft to be utilized in the intensification of the hailstorms.

These results do not fully confirm Dessen's (1960) finding that strong winds aloft determine whether or not a thunderstorm situation will transform itself into a heavy destructive hailstorm. Included in the present study are examples of heavy hailstorms occurring when the representative maximum winds aloft were as light as 27 knots. If hailstorms in the heavy hail category of this study could have been further stratified, to consider only rapidly-moving hailstorms accompanied by damaging squalls, then Dessen's findings would very likely have been strongly supported.

Schleusener and Auer (1964) studied wind profiles over North-eastern Colorado for days of "severe," "moderate," and "no hail" occurrence for the period 15 May-31 July, 1960-63. The average 200 mb wind for "severe" hail occurrence presented in their data was 47 knots. They cited a range of between 30 and 110 knots maximum wind. This compares with an average of 57 knots, and a range of between 27 and 92 knots maximum wind at 200 mbs found during the present study. The standard deviations from the averages presented in Figure 3 are typically large. The standard deviation for the average 200 mb windspeed of the present study was ± 18 knots.

A primary difficulty in the study conducted by Schleusener and Auer was a lack of success in finding a windspeed profile which would distinguish days of "moderate" and "no hail" occurrence. It

has been possible to show such a distinction in the present study because of the availability of improved hailfall data from the cooperative reporting network.

The results shown in Figure 3 of the present study do not agree with part of the findings of Ratner (1961). His data indicated that the magnitude of the winds aloft was apparently of no importance in determining hail occurrence. Ratner found that the maximum winds showed no preference for either hail days, or no hail days. Comparable mean maximum windspeeds from Ratner's study are shown in Figure 3.

In examining the windspeed profiles of Figure 3, it is to be noted that above 500 mb there is little difference in the slopes of the profiles for each of the hail intensity categories. This implies no appreciable variation in the vertical wind shear between categories for heights above 500 mb. Below 500 mb there is appreciable change in both windspeed and direction with height. It will be shown in the next section that most of the mean directional change takes place below 600 mb.

Mean Wind Direction Profiles for Northeastern Colorado

The mean wind direction profiles for the hail seasons of 1966, 1967, and 1968 are shown in Figure 4. The trend during this period was for the lower level winds to be from the southeast, or south, and then to shift sharply with increasing height to between southwest and west. The heavy hail profile shows a slightly more southwesterly direction than the remaining categories, which are more westerly in direction in the mean. The standard deviation in degrees from the average heavy hail direction at one representative level is shown in Figure 4.

Mean Vertical Wind Shear for the Hail Season of 1967

Mean vertical wind shears for the surface to 500 mb layer were computed by averaging the magnitudes of the shear vectors for individual days. The results, presented in Table 4, show the mean change of velocity, in any plane, with height in the lower half of the troposphere for the various categories of hail intensity. Also presented is a comparison of the magnitudes of upper level wind shear

for the 500-250 mb layer. A systematic increase of hail intensity
with increase of vertical wind shear was noted for the lower levels.
No such trend was apparent for the upper level shears, which showed
approximately the same shear magnitude for all of the hail intensity
categories.

The foregoing clearly shows that wind shear in the lower levels
was an important factor in the increased production of hail, while
the upper level shear was apparently not such an important factor.
The presence of higher windspeeds aloft, however, as previously shown,
was apparently also important for the increased production of hail.

In a comparable finding for upper level shear, referenced in
Table 4, Ratner (1961) shows shear to have an adverse effect on hail
production. Examination of the balance of the data from his 1961
paper, however, shows the maximum values of shear to have no preference
for either hail days, or no hail days.

Further evidence regarding the importance of low level shear is
apparent in the data of Table 5. This table presents certain mean
environmental winds at 600 and 500 mb for four categories of hail
intensity. It is to be noted that the shear in the 600-500 mb layer
is zero for the no hail category, and increases in magnitude with
increase of hail intensity.

From a physical point of view, the higher values of vertical wind
shear in the lower levels imply a marked veering of the environmental
wind; with higher windspeeds at the surface opposing in direction
higher windspeeds in the middle levels. The introduction of a moving
storm and its updraft-downdraft system into this sheared wind field
could place these air movements in direct opposition.

Classification of the Hail Season Days

The results of the classification of hail days of 1966, 1967, and
1968 are shown in Table 3. Of the three years, 1967 had the most hail
activity, and 1966 the least, as shown by the total number of hail and
no hail days. During the three year period analyzed, the data shows

that almost exactly half of the days experienced hailfall somewhere in the CSU hailstorm study area shown in Figure 1.

Mean Radar Echo and Storm Motion During the Hail Season of 1967

Table 5 presents a summary of mean hailswath direction and speed, mean radar echo motion, and the corresponding mean environmental winds for the summer of 1967. The radar echo mean speeds showed an increase of speed with increasing hail intensity. The standard deviations from the radar echo mean speeds are given for each hail intensity category.

The corresponding mean environmental winds have been included in Table 5 for comparative purposes. It appears that the environmental windspeeds between the 500 and 600 mb levels approximately match the radar echo speeds and the hailswath progression rates. This is in agreement with the findings of Schleusener and Grant (1961) for hailstorms in the northeastern Colorado area during 1961. These investigators found that hailswath tracks and radar echoes moved with a speed greater than the 14,000 foot windspeeds, and less than the 18,000 foot windspeeds.

How do the mean radar echo speeds measured in 1967 compare with the three-year mean environmental windspeeds of Figure 3 at the apparent steering level? Assuming that 550 mb is the steering level, the following comparison of mean environmental windspeeds to mean radar echo speeds, respectively, can be made: heavy hail, 23 kts versus 24 kts echo speed; moderate hail, 21 kts versus 24 kts; light hail, 15 kts versus 15 kts.

This comparison provides further indication of the close association of radar echo speeds and the middle level winds.

Thermally Induced Cloud Vertical Velocity Profiles

Figure 8 shows the mean profiles of the thermally induced component of cloud vertical velocity for the four hail intensity categories. The increase of vertical velocity with increase of hail intensity is clearly shown. This implies progressively steeper lapse rates, in the mean, with increase of hail intensity.

For the no hail-echoes category, profiles for both the undiluted parcel ascent condition, and an assumed dilution through entrainment condition have been shown for comparison. The diluted no hail-echoes profile shows the capability of barely supporting the maximum sized raindrops. The thermally induced component of cloud velocity for the undiluted no hail-echoes case was capable of supporting, at 450 mb, hail of approximately 1.2 cm in diameter, according to the $C_D = 0.5$ curve of Figure 11. This size will melt before reaching the ground, barring further growth between the zero isotherm and 450 mb. The light hail velocity profile could support, at 450 mb, hail of 1.8 cm diameter. This size would probably reach the ground unmelted, according to Ludlam (1958), and Sulakvelidze (1965), who showed that hail must be at least 1.5 to 2 cm in diameter at the zero isotherm level in order to reach the ground unmelted.

The moderate hail profile shows the capability of supporting hail 3 cm in diameter at 450 mb. The heavy hail profile is capable of supporting hail 3.7 cm in diameter, but no larger. Larger hail would have to be supported much higher in the cloud, according to these velocity profiles.

Hydrodynamically Induced Vertical Velocity Profiles

Figure 9 shows the mean profiles of the hydrodynamically induced component of cloud vertical velocity for the hail intensity categories. These profiles show the updraft vertical velocity structures which would be achieved if Newton's hypothesized mechanism of interaction between the cloud and the environment were operating alone without the thermally induced buoyancy. It is seen that these velocities are of the same order of magnitude as the thermally induced component. The profiles show that the heavy hail cases, in the mean, experienced the greatest degree of interaction with the environment, and the no hail-echoes cases experienced the least. Newton's hypothesized mechanism of interaction was explained in detail in the section on Procedure and Presentation of Results.

The profiles show a progressive increase of induced vertical velocity with increase of hail intensity for the levels below 400 mb. Above 400 mb, there is a relatively large difference between the no hail and the heavy hail profiles. The gradation between the light, moderate, and heavy hail profiles, however, is not as well defined for the upper levels of the cloud as it is for the lower levels.

The significant aspect of these profiles is that they clearly show the development of high vertical velocities of the magnitude required to assist the support of large hail at a lower level in the cloud. Nearly all of the hydrodynamically induced velocity has been achieved at the 700 mb level, which is before the thermally induced velocity becomes a factor.

It is therefore in the sub-cloud layer where Newton's hypothesized interaction mechanism has real importance. The vertical motions induced above cloud base by this mechanism are shown to be relatively insignificant. The motion of the storm provides the primary impetus for the interaction with the environment. The divergent outflow in the sub-cloud layer caused by thermodynamic processes within the storm provides additional impetus. The effect of marked directional shear of the environmental flow heightens the magnitude of the inter-action.

Combined Effect Cloud Vertical Velocity Profiles

Figure 10 shows the mean profiles of cloud vertical velocity for the various categories of hail intensity. These vertical velocities are due to the combined effect of the thermally and hydrodynamically induced buoyant accelerations. The profiles show progressively higher vertical velocities with increasing hail intensity. The pro-file for no hail-echoes, which had been reduced by entrainment, is shown for comparison. Both the parcel ascent, and the diluted profile are nearly the same at the lower levels of the cloud. Only above 450 mb are the profiles significantly different. Thus in this analy-sis, entrainment considerations for the full cloud depth would not greatly affect the vertical velocities developed in the lower levels.

The total updraft vertical velocity profile for the no hail-echoes cases, reduced by entrainment, is not capable of supporting hail which will reach the ground unmelted from any level. The no hail-echoes undiluted vertical velocity profile does have the capability of supporting a 2.1 cm hailstone at 450 mb. As previously indicated, this size would probably reach the surface unmelted.

The light hail profile now has the capability of supporting a 3.5 cm diameter hailstone at 450 mb. The moderate hail profile with a 39 mps velocity at 450 mb, can now support a 5.0 cm diameter hail-stone. The heavy hail profile velocity would now support a hailstone of 5.7 cm, or approximately 2.3 inches in diameter, at 450 mb, according to Figure 12.

How realistic are these profiles? Measurements made in updrafts at cloud base by aircraft of the CSU hail modification project have, on occasion, been of the magnitude indicated in Figure 11. Auer and Sand (1965) cite measurements of 22.5 mps, and 17.5 mps, made for short periods under heavily-precipitating cumulonimbus clouds. Sub-sequent observations of similar magnitude have been made.

These observations suggest the validity of the derived vertical velocity profiles presented in this paper.

The Effect of Precipitation Accumulations on Cloud Vertical Velocity

It has been shown that the combination of thermal and hydro-dynamic effects provided the updraft velocity of sufficient magnitude to support large hail in the 500-400 mb layer in the storm cloud mass. The hydrodynamic effects are contingent upon a well developed down-draft system, which implies that precipitation has existed within the cloud for some time. The cloud vertical velocity profiles presented in Figure 10 represent the achievement of near parcel ascent condition velocities. At this stage, it is reasoned, precipitation formed during previous updraft ascents may be descending into newly ascending up-drafts. The process of continuing collection of precipitation by new updrafts eventually results in the dampening of updraft velocities

due to the accumulated load of precipitation. The cloud velocity profile presented in Figure 10 is perhaps only transiently realizable. It is the result of repeated updraft ascents into a particular volume. It is prior, however, to appreciable accumulation of precipitation in this volume.

Observation of radar echo reflectivity aloft have provided evidence of the existence of a hail and precipitation accumulation zone at a level below 25,000 feet. In order for hail or rain to remain in this zone, the updraft velocity must decrease rapidly with height above the level of maximum velocity. If not, the particles would be elevated, along with the height of the reflectivity maximum.

Figure 12 shows the effect of several assumed hail and precipitation loads concentrated between 400-500 mb on a typical heavy hail updraft profile. Note that thermal buoyancy forces were still present above the accumulation zone and tended to re-accelerate the dampened updraft. The accumulations of 2 and 5 cm diameter hailstones at the concentrations suggested by Ludlam (1958), had a nearly negligible effect on the vertical velocity profile. The concentration of 2 mm diameter raindrops at a liquid water c content of 10 $g.M^{-3}$ did not produce the negative slope of the modified velocity profile required to effectively trap the precipitation particles in the accumulation region. Any precipitation load equalling, or exceeding the equivalent force of the updraft, could modify the velocity profile such that the precipitation particles would be effectively trapped. With knowledge of the updraft acceleration factor A_C for the layer, an equivalent precipitation concentration in $g.M^{-3}$ of liquid water can be calculated. In this case, 31 $g.M^{-3}$ or more of liquid water equivalent would suffice.

Thus it is shown that reasonable values of precipitation concentrations can produce a dampened updraft vertical velocity profile capable of suspending, but not elevating, large size hailstones at a low level in the cloud.

IV. CONCLUDING REMARKS

General Conclusions

There is a clear trend of increasing windspeed magnitudes aloft with increase in hail production, indicating that higher winds aloft, especially in the middle levels, may be an important factor in the production of hail. The magnitudes of the winds aloft serve as an index of the amount of kinetic energy potentially available for lifting low level air layers during storm activity.

There is a clear trend of increasing storm migration speed with increase in hail production. Storm migration speed in this region appears to roughly match the middle level winds.

Computed values of mean vertical wind shear for the levels above 500 mb were approximately the same for all categories of hail intensity. Upper level shear, therefore, was not an important factor in the production of hail. Below 500 mb, computed wind shear showed a systematic increase with increase in hail production, indicating that lower level wind shear is an important factor in hail production.

It is near the surface where Newton's hypothesis of a hydrodynamic interaction mechanism was found to be important for hailstorms in Northeastern Colorado. The effect aloft has been shown to be insignificant.

In order to find general agreement with the radar reflectivity profiles which are believed to show the location of precipitation particle growth zones at the level of maximum reflectivity, vertical velocities sufficient to support large hail must exist at that level. It has been shown in this paper that thermal buoyancy alone appeared incapable of providing the vertical velocities required to support large hail at the 500 - 400 mb level.

It has been further shown that the process of hydrodynamic interaction of the moving storm and a vertically sheared wind environment is capable of producing vertical velocities sufficient to support large hail at a lower level in the cloud.

The model of a hailstorm structure capable of accumulating hail in the lower middle of the cloud requires a vertical velocity maximum beneath the hail zone in order to prevent hail from being elevated into regions of normally greater vertical velocity aloft. It has been shown that the superposition of reasonable concentrations of hail and precipitation upon updraft velocity profiles derived from actual cases indeed produce such profiles.

Recommendations for Future Research

The present research has examined the influence of the unperturbed wind field on developing hailstorms. The interaction of a moving hailstorm with the lower level environmental wind was shown to be an important factor in the further development of the storm. The assumption was made in this study that the unperturbed winds directly impinged on the storm masses. Several important questions of relevancy are: what effect does the developing storm have on the environmental wind field? What is the possible role of the storm in inducing convergent circulation systems beneath the storm? How is the interaction mechanism, as presently envisioned, affected by perturbation of the environmental winds?

It is therefore recommended that future research focus upon the interaction of the storm with the subcloud environment in greater detail, with emphasis on the effect of the developing storm on the environment.

V. REFERENCES

Atlas, D., 1963: Radar analysis of severe storms. Severe Local Storms. Meteor. Monograph 5, No. 27, Boston, Amer. Meteor. Soc., 177-220.

Auer, A. H., Jr. and W. Sand, 1966: Updraft measurement beneath the base of cumulus and cumulonimbus clouds. J. Appl. Meteor., 5, 461-466.

Austin, J. M., 1948: A note on cumulus growth in a nonsaturated environment. J. Meteor., 5, 103-107.

Beckwith, W. B., 1956: Hail observations in the Denver area. United Air Lines, Meteor. Circ. 40, 41 pp.

Beckwith, W. B., 1960: Analysis of hailstorms in the Denver network, 1949-1958. Physics of Precipitation, Geophys. Monogr. No. 5, Washington, D. C., Amer. Geophys. Union, 348-353.

Browning, K. A. and F. H. Ludlam, 1962: Airflow in convective storms, Quart. J. R. Meteor. Soc., 88, 117-135.

Bilham, E. G. and E. F. Relf, 1937: The dynamics of large hailstones. Quart. J. R. Meteor. Soc., 63, 149-162.

Byers, H. R., 1959: General meteorology. New York, McGraw-Hill Book Company, 188-190.

Byers, H. R. and L. J. Battan, 1949: Some effects of vertical wind shear on thunderstorm structure. Bull. Amer. Meteor. Soc., 30, 168-175.

Byers, H. R. and R. R. Braham, 1949: The Thunderstorm. Washington, D. C., U. S. Government Printing Office, 287 pp.

Das, P., 1962: Influence of wind shear on the growth of hail. J. Atmos. Sci. 19, 407-414.

Dessens, H., 1960: Severe hailstorms are associated with very strong winds between 6000 and 12,000 meters. Physics of Precipitation, Geophys. Monogr. No. 5, Washington, D. C., Amer. Geophys. Union, 333-338.

Dessens, H., 1961: Comments on "Do high speed winds aloft influence the occurrence of hail?" Bull. Amer. Meteor. Soc., 42, 513.

Donaldson, R. J., 1961: Radar Reflectivity profiles in thunderstorms. J. Meteor. 18, 292-305.

Ference, M., Jr., 1951: Instruments and techniques for meteorological measurements. Compendium of Meteorology. Boston, Amer. Meteor. Soc., 1207-1209.

Fischer, R. E., 1968: Personal communication, Colorado State University.

Goldstein, S. (Editor), 1938: Modern developments in fluid mechanics. New York, Dover Publications (702 pp.).

Gunn, R. and G. D. Kinzer, 1949: The terminal velocity of fall for water droplets in stagnant air. J. Meteor. 6, 243-248.

Hitschfeld, W., 1960: The motion and erosion of convective storms in severe vertical wind shear. J. Meteor., 17, 270-282.

Hoerner, S., 1958: Fluid dynamic drag. New York, published by the author, 203 pp.

Huschke, R. E., 1959: Glossary of meteorology. Boston, Amer. Meteor. Soc. 638 pp.

Iribarne, J. V., 1968: Development of accumulation zones. Proceedings of the International Cloud Physics Conference Toronto, 350-355.

Levine, J., 1959: Spherical vortex theory of bubble-like motion in cumulus clouds. J. Meteor., 16, 653-662.

List, Robert J., 1949: Smithsonian meteorological tables. Washington, D. C., Smithsonian Institution.

List, Roland J., 1961: On the growth of hailstones. Nubila, Anno IV, 29-38.

Longley, R. W., and C. E. Thompson, 1965: A study of the causes of hail. J. Appl. Meteor., 4(1), 69-82.

Ludlam, F. H., 1958: The hail problem. Nubila, 1, 12-96.

Ludlam, F. H., 1963: Severe local storms: a review. Severe Local Storms, Meteor. Monograph, 5, No. 27, Boston, Amer. Meteor. Soc., 1-30.

Ludlam, F. H., 1966: Cumulus and cumulus convection. Tellus 4, 687-698.

Ludlam, F. H. and W. C. Macklin, 1959: Some aspects of a severe storm in the S. E. England. Nubila, Anno II, 38-50.

APPENDIX

List of Symbols

A = any vertical acceleration.

A_C = vertical acceleration of a cloud updraft column due to all buoyant effects.

A_C' = vertical acceleration of a cloud updraft column modified to include the effects of an imposed accumulation of large precipitation particles.

A_H = vertical acceleration of an updraft column due to all wind shear induced hydrodynamic effects.

$A_H' = g\frac{\partial H}{\partial P_e}$: the vertical acceleration of an updraft column due to the reduction of non-hydrostatic pressure with height.

$A_N = g\frac{H}{P}$

A_p = deceleration of an updraft column due to the drag of an imposed accumulation of large precipitation particles.

A_T = vertical acceleration of a cloud updraft column due to a horizontal temperature difference between updraft and environment.

A_T' = the term A_T modified by the inclusion of entrainment considerations.

C_D = the drag coefficient for the flow of updraft air about a precipitation particle.

D = storm diameter.

d = the precipitation particle diameter.

F = drag force on the precipitation particles; equivalent to the retarding force on the updraft.

g = the acceleration of gravity.

$H = K\,1/2\rho V_R^2$: the non-hydrostatic pressure at any point on the cloud periphery at a given level.

K = the hydrodynamic pressure coefficient.

M = unit mass of 1 kg.

N = the number of precipitation particle in the volume occupied by a unit mass of updraft.

P = total pressure of an updraft column; i.e., the hydrostatic pressure plus the non-hydrostatic (hydrodynamic) pressure.

P_e = pressure of the environment.

P_h = hydrostatic pressure component of P.

List of Symbols (continued)

R_e = Reynolds Number.

T = temperature of the updraft.

T_e = mean layer temperature of the environment.

u = the zonal component of wind velocity.

v = the meridional component of wind velocity.

V_1 = initial vertical velocity of the updraft at the base of a layer of integration.

V_2 = final vertical velocity at the top of the layer.

V_C = mean in-cloud horizontal velocity.

V_e = environmental wind velocity.

V_R = relative wind velocity with reference to a moving storm.

V_T = terminal velocity of precipitation particles.

w = the vertical component of wind velocity.

Z_1 = vertical coordinate of the base of a layer of integration.

Z_2 = vertical coordinate of the top of the layer.

ΔT = the temperature difference between the updraft and its environment.

ρ_a = the density of the updraft at a given level.

ρ_e = the density of the environment at a given level.

ρ_i = hailstone density.

μ = the kinematic viscosity of air.

$\frac{\partial u}{\partial P}$ = vertical shear of the zonal wind expressed in pressure coordinates.

$\frac{\partial v}{\partial P}$ = vertical shear of the meridional wind expressed in pressure coordinates.